metals

MDPI

Review

Research Progress on Solvation Sheath Regulation Additives in $ZnSO_4$ Electrolytes for Aqueous Zinc-Ion Batteries

Biao Wang [1,2] and Yongsheng Ren [1,2,*]

[1] School of Metallurgical and Energy Engineering, Kunming University of Science and Technology, Kunming 650093, China; 13211899688@163.com
[2] State Key Laboratory of Complex Nonferrous Metal Resources Clean Utilization, School of Metallurgical and Energy Engineering, Kunming University of Science and Technology, Kunming 650093, China
* Correspondence: ryssdy@126.com

Abstract

Aqueous zinc-ion batteries (AZIBs) are promising for scalable energy storage, yet their practical viability is constrained by zinc dendrite propagation, parasitic hydrogen evolution, and interfacial corrosion. Formulating electrolyte additives represents an economically viable strategy to address these long-standing bottlenecks by modulating the bulk solution and double-layer environments. Diverging from traditional composition-based classifications, this review categorizes recent additive strategies according to their underlying physical chemistry mechanisms. Specifically, we evaluate how these additives regulate the primary and secondary Zn^{2+} solvation sheaths, reconstruct the electric double layer (EDL) for crystallographic facet control, induce sacrificial or mineralized solid electrolyte interphases (SEIs), and establish responsive polymer confinement networks. Furthermore, we critically discuss the operational limitations, trade-offs, and parameter dependencies of these strategies under non-ideal, realistic conditions. Finally, prospective directions are outlined—focusing on descriptor-driven design, operando non-equilibrium characterizations, and performance validation under standard industrial metrics (e.g., low E/C ratios and high depths of discharge)—to provide an objective framework for advancing electrolyte optimization in practical zinc-based energy storage.

Keywords: aqueous zinc-ion batteries; electrolyte additives; solvation structure; electric double layer; interfacial mechanisms; practical operating metrics

1. Introduction

The global transition toward sustainable energy storage has intensified research into alternatives to lithium-ion batteries (LIBs), which face geopolitical resource constraints and safety concerns [1–15]. Aqueous zinc-ion batteries (AZIBs) utilizing mild $ZnSO_4$ electrolytes offer competitive advantages, including a high theoretical volumetric capacity (5854 $mAh \cdot cm^{-3}$), a suitable redox potential (−0.762 V vs. SHE), and environmental compatibility [16–27]. However, achieving high reversibility under practical operating regimes remains a long-standing challenge. Fundamental issues at the zinc/electrolyte interface—such as dendrite proliferation, parasitic hydrogen evolution reaction (HER), and surface corrosion—are not recent discoveries; they have been recognized for decades, dating back to early alkaline and neutral zinc battery studies [e.g., Dirkse, 1966]. These interconnected degradation pathways drastically limit the lifespan and zinc utilization efficiency of the anodes under non-ideal, realistic configurations [28–34].

Check for updates

Academic Editor: Henrik K. Hansen

Received: 1 June 2026
Revised: 23 June 2026
Accepted: 27 June 2026
Published: 12 August 2026

Copyright: © 2026 by the authors. Licensee MDPI, Basel, Switzerland. This article is an open access article distributed under the terms and conditions of the Creative Commons Attribution (CC BY) license.

Among various remediation strategies, incorporating targeted electrolyte additives represents an economically viable and scalable approach to modulate interfacial chemistry without requiring complex electrode restructuring [35–42]. Moving away from descriptive classifications based strictly on chemical composition, this review categorizes recent additive strategies according to their underlying physical chemistry mechanisms. We critically evaluate how additives regulate the primary and secondary Zn^{2+} solvation sheaths, restructure the electric double layer (EDL) for crystallographic facet control, induce sacrificial or mineralized solid electrolyte interphases (SEIs), and establish responsive polymer network architectures. Special emphasis is placed on identifying the operational limitations, trade-offs, and dependencies on testing parameters (such as electrolyte volume and depth of discharge) inherent to these strategies. By synthesizing these mechanistic insights alongside their practical constraints, this framework aims to serve as an objective reference to guide the rational optimization of electrolytes for viable zinc-based energy storage.

2. Key Bottlenecks and Failure Mechanisms of $ZnSO_4$ Electrolyte

The interfacial instability, slow charge-transfer kinetics, and parasitic side reactions governing zinc electrodes are not unique to modern aqueous zinc-ion batteries (AZIBs) [43–48]. Historically, as pioneered by Dirkse (1966) in early studies on alkaline and neutral zinc systems, foundational transport limitations, passivation, and chemical corrosion have long been recognized as severe bottlenecks for zinc-based electrochemistry [49–51]. In contemporary mild $ZnSO_4$ systems, these degradation pathways remain intertwined, heavily depending on operating parameters such as current density, localized pH variations, and electrolyte concentrations [52–54].

Thermodynamic Limitations & Parasitic Reactions: The narrow theoretical electrochemical stability window of water (1.23 V) inherently restricts the operational voltage of aqueous systems [55,56]. Within mild $ZnSO_4$ electrolytes, active free water molecules in the primary solvation sheath readily undergo the parasitic hydrogen evolution reaction (HER) under cathodic polarization. This localized reduction consumes protons, causing a significant upward drift in the interfacial pH [57]. Consequently, insulated byproducts like zinc hydroxide ($Zn(OH)_2$) and zinc sulfate hydroxide hydrates ($Zn_4SO_4(OH)_6 \cdot xH_2O$, ZHS) precipitate onto the electrode surface, driving active area decay and capacity fading [58,59].

Mass Transport & Solvation Kinetics: Active zinc ions predominantly exist as the bulky hexaaqua-zinc complex ($[Zn(H_2O)_6]^{2+}$), which exhibits a high desolvation free energy [60,61]. This solvation shell imposes a substantial kinetic barrier for charge transfer at the phase boundary. Simultaneously, the large hydrodynamic radius and high charge density of SO_4^{2-} anions retard their migration within the bulk solution [62–68]. Under severe polarization or high-rate operations, these mismatched transport velocities trigger pronounced localized concentration gradients. This exacerbates concentration polarization and lowers the overall ionic conductivity [69–71].

Morphological Degradation (Dendrite Growth): Uncontrolled zinc dendrite propagation is fundamentally governed by non-uniform local electric fields and restricted mass transport [72–74]. During electrodeposition, the uncompensated transport flux causes spatial variations in Zn^{2+} availability across the anode surface [75,76]. This non-uniformity initiates the "tip effect," wherein localized current crowding accelerates deposition at microprotrusions. Notably, these failure modes are sensitive to electrolyte concentration: dilute formulations aggravate mass-transport polarization due to local ion deficiency, whereas excessively concentrated regimes induce severe viscosity-driven diffusion resistance, both of which accelerate premature short-circuits [77–79].

3. Zinc Sulfate Electrolyte Additives

Incorporating electrolyte additives provides a practical approach to alter the physicochemical properties of $ZnSO_4$ electrolytes without requiring complex electrode restructuring [80,81]. By managing bulk or interfacial microenvironments, these low-concentration formulations can suppress parasitic side reactions like HER and facilitate uniform zinc deposition [82,83]. To address the overlapping definitions inherent to traditional composition-based groupings (which frequently conflate organic, inorganic, molecular, and ionic categories), this section systematizes recent research progress based strictly on their primary physical chemistry mechanisms [84,85]. Specifically, additive strategies are evaluated through four progressive regulatory domains: bulk and secondary Zn^{2+} solvation sheath modulation, electric double layer (EDL) reconstruction for crystallographic control, sacrificial reduction and inorganic mineralization for solid electrolyte interphase (SEI) construction, and the assembly of responsive polymer confinement networks.

3.1. Solvation Chemistry Modulation

Solvation chemistry modulation serves as a fundamental pillar for suppressing parasitic side reactions in aqueous zinc-ion batteries (AZIBs). In conventional dilute electrolytes, Zn^{2+} exists as the classical hydrated zinc ion $[Zn(H_2O)_6]^{2+}$, wherein the highly active coordinated water molecules easily trigger the hydrogen evolution reaction (HER) and chemical corrosion during desolvation. Introducing organic molecules or inorganic anions with potent coordinating capabilities into the primary or secondary solvation sheaths of Zn^{2+} to displace or anchor detrimental free water can thermodynamically widen the electrochemical stability window and effectively lower the desolvation kinetic barrier, guiding a uniform zinc flux distribution [86].

To achieve precise control over the solvation sheath, the academic paradigm is transitioning from empirical "trial-and-error" screening to rational design based on quantitative quantum chemical descriptors. Generally, the lowest unoccupied molecular orbital (LUMO) energy level of a molecule dictates its electron-accepting capability, where a lower LUMO favors preferential sacrificial reduction at the anode surface to construct a solid electrolyte interphase (SEI) film. Conversely, the highest occupied molecular orbital (HOMO) energy level governs the electron-donating coordination and adsorption behavior; a higher HOMO energy level indicates a stronger coordination affinity toward Zn^{2+}, enabling effective displacement of bound water within the primary solvation shell [87].

For small-molecule electrolyte additives, utilizing the strong coordination of specific functional groups to reconstruct local solvation networks has yielded significant progress. Wang et al. [88] introduced an ethane sulfonamide (ESA) organic additive featuring a zinc-loving sulfonamide group ($-SO_2NH_2$) (Figure 1a). This group works synergistically with a hydrophobic alkyl chain to reshape the bulk Zn^{2+} solvation shell, subsequently transforming into a dense SEI film with high Zn^{2+} conductivity and strong mechanical barrier performance at the phase interface, enabling an average coulombic efficiency (CE) of 99.92% at a high current density of 5 $mA \cdot cm^{-2}$. Similarly, Zhai et al. [89] reported a tetrahydrofurfuryl alcohol (THFA) additive possessing dual hydrogen-bond regulation sites consisting of hydroxyl (-OH) and ether (-C-O-) bonds (Figure 1b). THFA suppresses bulk water activity through its unique dual-site anchoring effect, while its oxygen atoms deeply penetrate the primary solvation shell of $[Zn(H_2O)_6]^{2+}$ to optimize desolvation resistance and effectively inhibit vanadium dissolution from the cathode side. With an adjustment of only 2%, it substantially extends the lifespan of symmetric cells from 150 h to 8800 h.

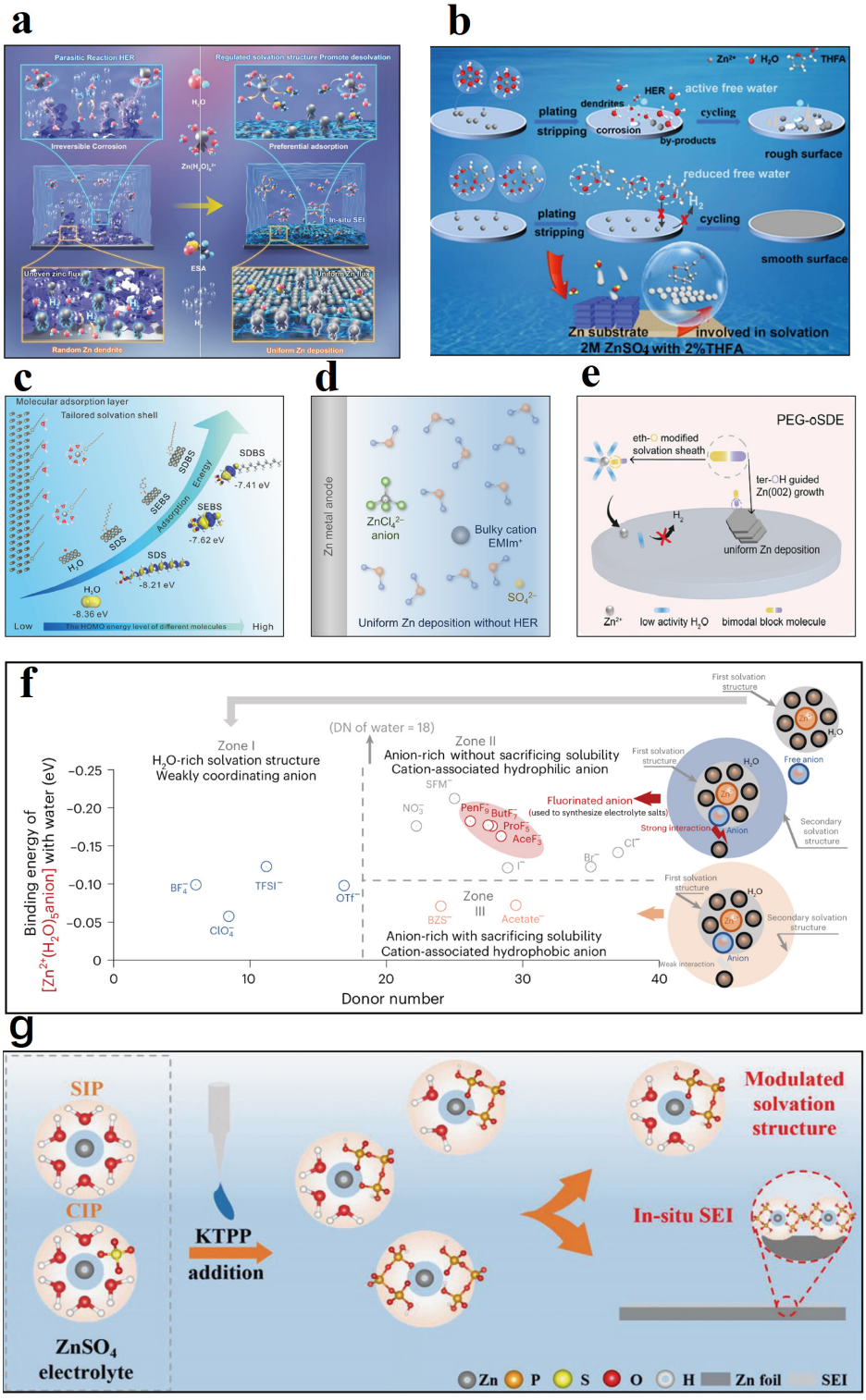


Figure 1. (**a**) Schematic illustration of Zn deposition behaviors in the electrolytes before (**left**) and after (**right**) ESA modification. Reprinted with permission from ref. [88]. 2023, Wiley. (**b**) Zn^{2+} ion behaviors during plating and stripping in ZS and THFA-ZS electrolytes. The THFA-ZS additive significantly inhibits side reactions and the formation of Zn protrusions. Reprinted from Ref. [89]. (**c**) Non-sacrificial anionic surfactant additives. Reprinted with permission from ref. [90]. 2024, Elsevier. (**d**) Schematic illustration of the anion-type water-free $[ZnCl_4]^{2-}$ solvation structure enabled by bulky cation chloride salt for dendrite-free Zn anodes. Reprinted with permission from ref. [91]. 2021, Wiley. (**e**) Proposed mechanism of the bimodal block molecule MA with oxygen species in different chemical environments in the electrolyte, which serves distinct roles in enhancing the electrochemical performance of the ZIBs. Reprinted with permission from ref. [92]. 2024, Wiley.

(**f**) Anion design principle for the formulation of aqueous electrolyte solutions. Reprinted with permission from ref. [93]. 2026, Springer Nature. (**g**) Schematic illustration of the working mechanism of the trifunctional KTPP electrolyte additive. Reprinted with permission from ref. [94]. 2023, Wiley.

By finely tuning the electron-donating coordination activity of additives, the charge property of solvation clusters can be thoroughly altered. Hu et al. [90] established a scientific screening paradigm using the HOMO energy level as a universal quantitative descriptor, successfully identifying the non-sacrificial anionic surfactant sodium dodecyl benzene sulfonate (SDBS) (Figure 1c). Exhibiting strong electron-donating coordination activity due to its high HOMO energy level, the sulfonate head of SDBS competitively displaces coordinated water in the bulk phase to optimize zinc ion transport, while forming a dense dynamic adsorption layer at the interface that leads to a stable symmetric cell lifespan exceeding 3200 h. While anionic surfactants optimize the environment on the outer periphery, highly coordinated chloride ions enable a deeper structural reorganization. Zhang et al. [91] introduced 1-ethyl-3-methylimidazolium chloride ([EMIM]Cl), an ionic liquid additive rich in bulky cations (Figure 1d). The highly coordinated Cl^- severs traditional Zn^{2+}-H_2O interactions, reversing the cationic hydrated zinc $[Zn(H_2O)_6]^{2+}$ into an anhydrous anionic complex $[ZnCl_4]^{2-}$. This fundamental reversal of charge properties eliminates the attack of active water; furthermore, the negatively charged $[ZnCl_4]^{2-}$ complexes spontaneously migrate away from the negatively charged zinc microprotrusions via electrostatic repulsion during deposition, redirecting the zinc flux toward flat regions and yielding a capacity retention of 78.8% after 300 polarizations in an anode-free configuration.

As the discipline progresses toward multi-functional and multi-dimensional protection, the long-chain topologies of polymers and the steric hindrance effects of composite inorganic anion networks have become key instruments for modulating solvation chemistry. Zhao et al. [92] addressed the issue of active free water in ultra-dilute systems by introducing a polyethylene glycol (PEG) macromolecular additive rich in bimodal active oxygen sites (Figure 1e). The ether oxygen (eth-O) atoms on the macromolecular backbone act as strong coordination centers to efficiently chelate Zn^{2+} and break down the bulk water hydrogen-bond network, while the terminal hydroxyl oxygen (ter-OH) atoms serve as zinc-loving adsorption modules that selectively bind to the thermodynamically unstable Zn(101) crystal plane. This steric hindrance effect forces the zinc flux to undergo directional two-dimensional growth along the flat Zn(002) plane, allowing full cells to retain 82% of their capacity after 1500 cycles. To further suppress free water under practical low-salt thresholds, Dong et al. [93] proposed a "Secondary Solvation Sheath" engineering strategy (Figure 1f). They introduced fluorinated anions with high donor numbers (DN > 18) to deeply penetrate the primary solvation shell of Zn^{2+}, forming $[Zn(H_2O)_5\text{-anion}]^{2+}$ nanoclusters. These coordinating anions cleverly act as "molecular bridges" to firmly anchor free water molecules within the secondary solvation shell and bulk phase through strong interactions. During electrodeposition, these fluorinated anions drift synchronously with the zinc flux to the anode boundary and undergo preferential sacrificial reduction, in situ cultivating a protective SEI film rich in inorganic ZnF_2 and delivering a prominent average CE of 99.99% at 1.5 $mA{\cdot}cm^{-2}$. Similarly, Yu et al. [94] incorporated a trifunctional inorganic oligomer, pentapotassium triphosphate (KTPP), into a baseline $ZnSO_4$ electrolyte (Figure 1g). This oligomer unfolds an efficient defensive sequence: the dissociated K^+ cations act as a dynamic electrostatic shield to blunt the "tip effect," while the highly negatively charged TPP^{3-} oligomeric anions aggressively coordinate with Zn^{2+}, displacing bound water molecules in $[Zn(H_2O)_6]^{2+}$ to form novel anionic complexes like $[Zn(H_2O)_3TPP]^-$. This process concurrently prompts a highly conductive and mechanically resilient inorganic SEI, driving an exceptional 3800-h symmetric cell lifespan and enabling the successful construction of a practical 9-mAh four-layer pouch cell.

3.2. EDL Engineering & Crystallographic Control

The electric double layer (EDL) is a critical frontier for modulating mass transport and nucleation kinetics at the anode–electrolyte interface. Due to the accumulation of active water molecules within the inner Helmholtz plane (IHP) and the non-uniform distribution of the local electric field, the zinc anode surface is highly susceptible to localized hydrogen evolution reaction (HER) and disordered dendrite growth. Introducing specifically adsorbed molecules, electrostatically shielding cations, or interfacial pH buffer pairs into the EDL can effectively reshape the potential distribution within the interfacial microenvironment, regulate local ionic fluxes, and guide Zn^{2+} to undergo layered epitaxial growth along specific low-energy crystal planes, such as the Zn(002) basal plane. This organic integration of EDL engineering and crystallographic control represents a pivotal approach to achieving low-polarization, dendrite-free zinc deposition under practical operating conditions [95–99].

To mitigate the parasitic HER within the acidic regions of the interface, Lin et al. [100] introduced triazole (Ta), a five-membered nitrogen heterocyclic molecule featuring a pi-electron conjugated system (Figure 2a). Profiting from its robust metal coordination capability and inherent proton-buffering mechanism, Ta spontaneously constructs a dynamically adsorbed molecular barrier on the zinc foil surface. This protective layer leverages the high electron mobility of the large conjugated plane to homogenize the local ion flux, guiding zinc to crystallize orderly along the lowest-energy facet and maintaining stable cycling for over 400 h at a high depth of discharge (DOD) of 85%. To balance the global stability of both the anode and cathode sides, Wang et al. [101] incorporated D-xylose (DX), a biomass small molecule rich in polar hydroxyl groups (Figure 2b). DX not only suppresses zinc flux aggregation and side reactions via characteristic adsorption on the anode side, but its adsorption at the cathode interface also significantly accelerates charge transfer and increases reactive sites, endowing the Zn||textMnO$_2$ full cell with excellent rate capability. With the rise of green chemistry, natural biomass macromolecules have garnered attention due to their unique architectures. Li et al. [102] innovatively utilized the natural polymer chitosan (CHI) as an electrolyte modifier (Figure 2c), exploiting the highly polar groups on its backbone to undergo spontaneous, dynamic adsorption and entanglement on the zinc foil and newly deposited layers. This dynamic protective layer effectively shields free water, while the chelating groups on its chain segments establish an efficient "capture–diffusion–deposition" pathway for ion transport, allowing the symmetric cell to operate stably for over 1380 h under a high flux of 10 mA·cm^{-2}.

In cation-mediated interface regulation paradigms, utilizing positively charged groups to respond to the cathodic electric field for constructing a dynamic electrostatic shielding layer is a classic method to eliminate the "tip effect". Gan et al. [103] introduced a long-chain cationic surfactant, hexadecyltrimethylammonium hydrogen sulfate CHN(HSO_4) (Figure 3a). A notable feature of this work is that at an ultra-trace concentration of only 0.01 mM, the dissociated CHN^+ cations can precisely target microprotrusions on the zinc surface to guide uniform Zn^{2+} nucleation via effective electrostatic shielding. Combined with the drainage network woven by its 16-carbon hydrophobic alkyl chains at the interface, it achieves a self-corrosion inhibition efficiency exceeding 90%. Furthermore, this traditional cation shielding mechanism has been refined by a recent in-situ microscopic diagnostic study. Yuan et al. [104] employed in-situ electrochemical liquid-phase transmission electron microscopy (LC-TEM) to visualize the real-time nanoscale nucleation trajectory of zinc upon the introduction of LiCl (Figure 3c). The study revealed that within the anisotropic lattice chemistry of aqueous zinc, the shielding effect of exogenous metal cations (such as Li^+) fundamentally acts as a "facet-selective regulator." It preferentially blocks the highly active Zn(100) step edges around embryonic zinc flakes through directional adsorption—which otherwise readily induce disordered dendrites—thereby forcing subsequent Zn^{2+} ions to

undergo continuous, layered epitaxial deposition exclusively on the flat Zn(002) basal surface. To maximize this cationic electrostatic repulsion, Cheng et al. [105] turned their attention to the high-valence tetravalent metal cation Zr^{4+} (Figure 3b). To address the spontaneous hydrolysis of high-valence cations in open aqueous systems, the authors immobilized them within a silk fibroin/polyacrylamide (SFPAM) hydrogel framework to restrict secondary hydrolysis. As an ionic modifier with an exceptionally high charge density, Zr^{4+} shortens the interfacial Debye length via its intense local electric field repulsion, forcing the zinc flux to pack tightly along the thermodynamically stable Zn(002) basal plane, enabling the symmetric cell to cycle robustly for over 1500 h at a severe temperature of −30 °C and a high DOD of 57%.

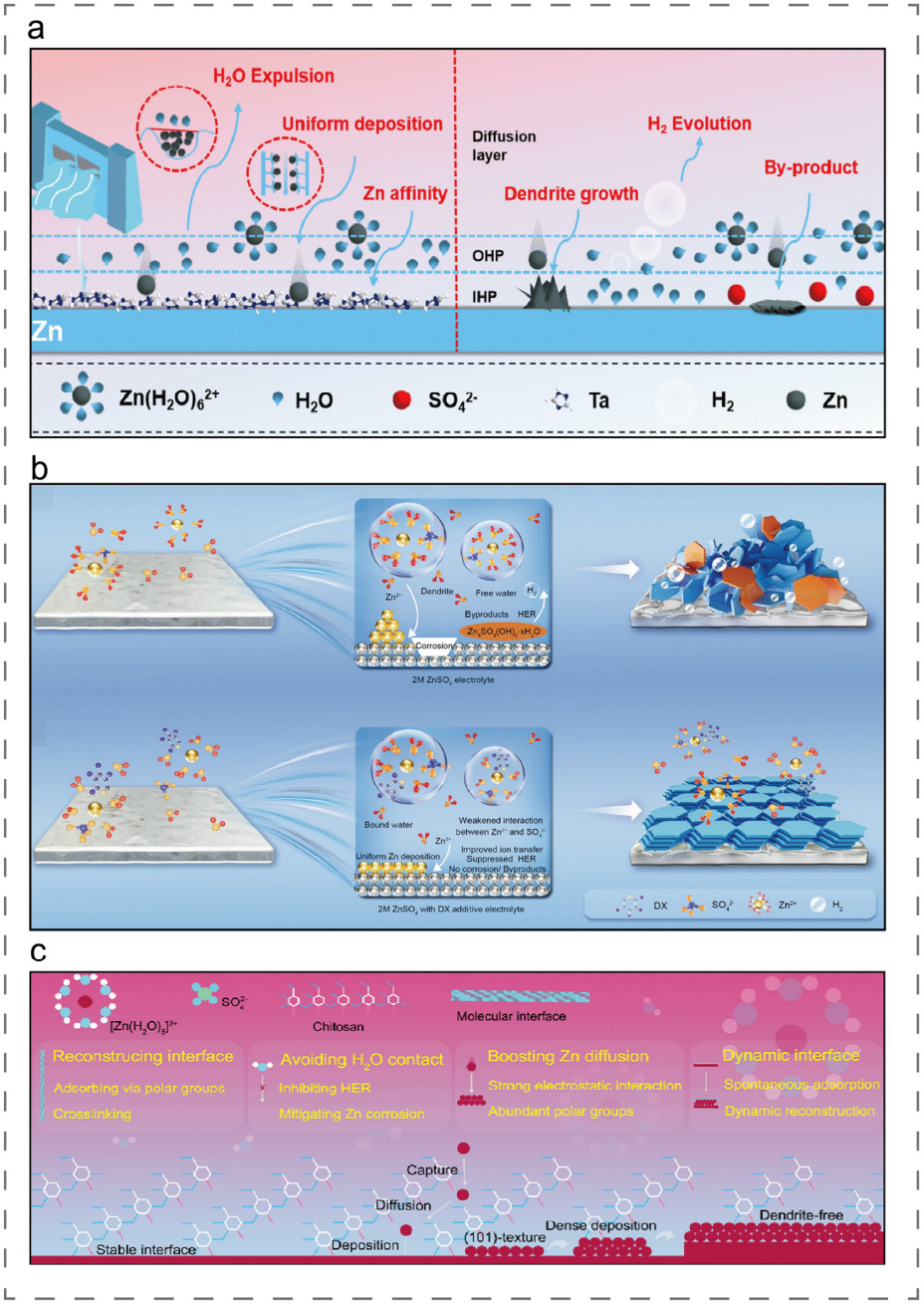


Figure 2. (**a**) Mechanism diagram of the Ta additive. Reprinted with permission from ref. [100]. 2013, Royal Society of Chemistry. (**b**) Diagram of the electroplating process of Zn^{2+} in electrolytes without and with DX. Reprinted with permission from ref. [101]. 2024, Wiley. (**c**) Schematic diagram of the function of CHI additives. Reprinted with permission from ref. [102]. 2025, Elsevier.

Beyond individual electrostatic shielding or molecular adsorption, restructuring complex ionic synergies and pH-buffering microenvironments can comprehensively enhance EDL tolerance against extreme conditions. Zhang et al. [106] introduced ammonium dihydrogen phosphate (NHP) into a dilute $ZnSO_4$ baseline system (Figure 3d), seamlessly integrating NH_4^+-mediated electrostatic shielding with an interfacial $NH_4^+/H_2PO_4^-$ pH buffer pair. This inorganic pair dynamically buffers protons at the phase boundary to suppress the localized alkalinity spike caused by parasitic hydrogen evolution, which, synchronized with electrostatic current homogenization, enables the cell to cycle stably for 930 h at a demanding current density of 10 $mA \cdot cm^{-2}$. Finally, to mitigate the drastic surge in interfacial impedance commonly encountered when ionic liquids are used as wide-temperature antifreeze agents, Yang et al. [107] introduced the "Hofmeister series" ion-specific effect into aqueous batteries, customizing a wide-temperature system characterized by "gradient chaotropic anions" composed of $Emim^+$ -TFA^-/OTf^--Zn^{2+}-H_2O (Figure 3e). Addressing the common problem of cryogenic ion transport blockage caused by the crowding of bulky hydrophobic $Emim^+$ cations in the EDL, the gradient-introduced disordered anions (TFA^- and OTf^-) disrupt the long-range ordered hydrogen-bond lattice of water in the bulk phase to inhibit ice crystallization. Concurrently, at the interface, they alleviate the steric hindrance and crowding of $Emim^+$ through sophisticated charge responses, constructing a low-impedance, "hydrophobic but salt-loving" EDL microenvironment on the anode surface. Benefiting from this holistic ionic reorganization, the zinc anode delivered enhanced durability in subzero environments, achieving over 13,000 h of stable stripping/plating at −30 °C and smooth operation exceeding 6690 h even under extreme cold at −40 °C.

3.3. Sacrificial Reduction & Inorganic Mineralization for SEI Construction

Constructing an artificial or in-situ solid electrolyte interphase (SEI) on the zinc anode surface represents a direct approach to isolating active water molecules and suppressing dendrite growth. Compared with interfacial modulators relying on physical adsorption, solid interphases constructed via electrochemical sacrificial reduction or chemical mineralization typically possess superior mechanical strength and lower phase-transfer impedance. This subsection focuses on modification strategies utilizing molecules with low lowest unoccupied molecular orbital (LUMO) energy levels for in-situ reductive filming, incorporating inorganic salts to manipulate crystallization thermodynamics, and employing solid nanoparticles to assemble cross-linked interfacial networks, aiming to elucidate how solid interphase engineering enables highly reversible and dendrite-free zinc deposition [108–111].

Utilizing small organic molecules with low LUMO energy levels, such as those bearing sulfonic acid or sulfonamide groups, to induce in-situ interfacial film formation is a representative paradigm for constructing rigid protective barriers. Li et al. [112] introduced trace amounts of sodium 4-aminobenzenesulfonate (SABS) into a baseline $ZnSO_4$ electrolyte (Figure 4a). Leveraging the zinc-loving properties of its amino and sulfonic acid groups, SABS preferentially adsorbs onto the anode surface, inducing the formation of a water-deficient inner Helmholtz plane (IHP). Due to the low LUMO energy level of SABS (−1.88 eV), it undergoes in-situ electrochemical reduction during cycling, transforming into an organic–inorganic hybrid SEI film. Under the synchronized protection of this reconstructed EDL and the in-situ formed interphase, the Zn||Zn symmetric cell achieved a stable lifespan of 6500 h at 1 $mA \cdot cm^{-2}$, and the assembled Zn||I_2 pouch cell maintained a capacity retention of 99.1% after 820 cycles.

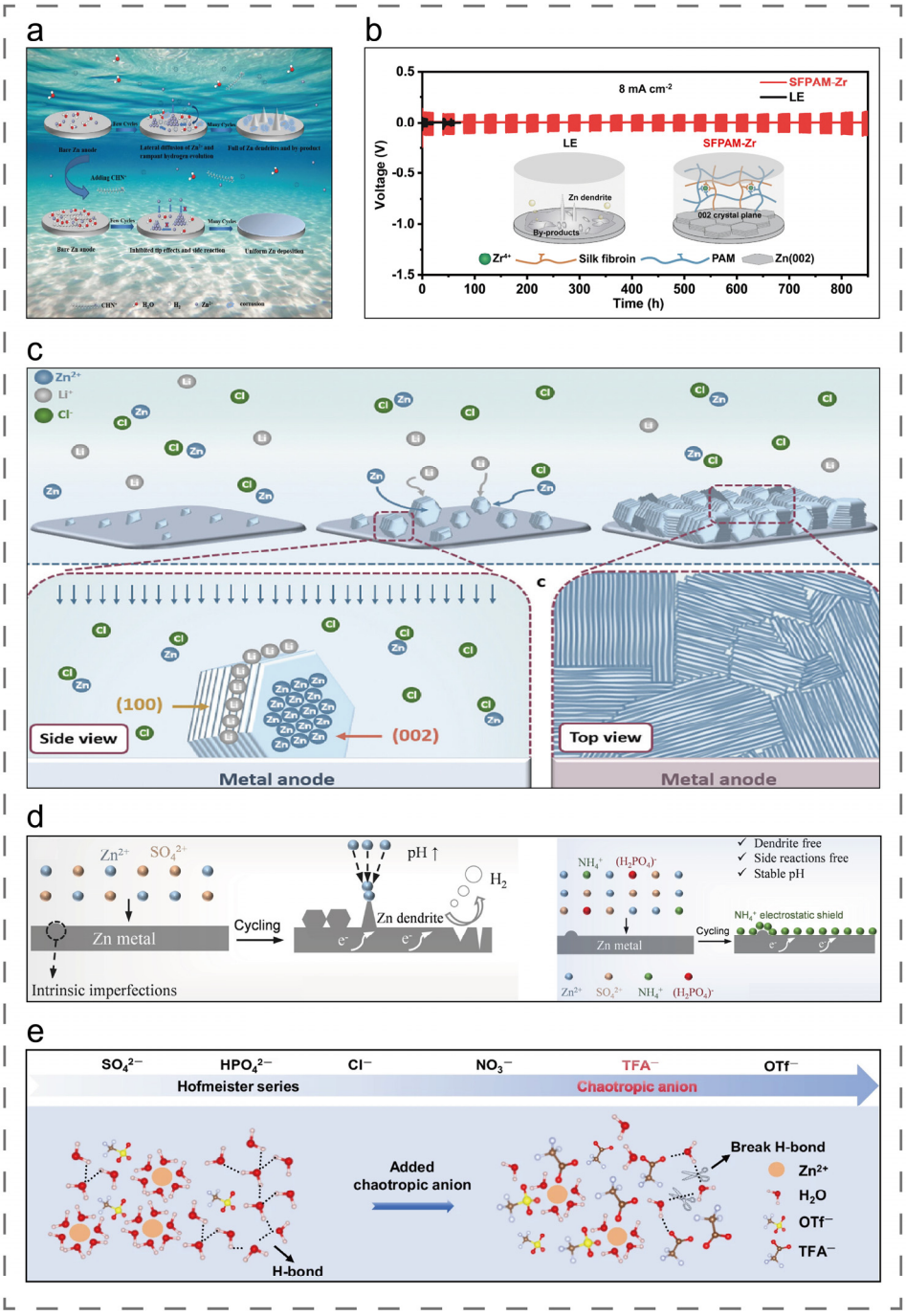


Figure 3. (**a**) Schematic illustration for comparing cyclic stability of Zn anode in 2 M $ZnSO_4$ without $CHN(HSO_4)$ and with $CHN(HSO_4)$. Reprinted with permission from ref. [103]. 2023, Elsevier. (**b**) A Zr^{4+} crosslinked hydrogel electrolyte is demonstrated on side reaction resistance for high-performance aqueous Zn-based devices. Reprinted with permission from ref. [105]. 2008, Royal Society of Chemistry. (**c**) Schematic illustration of the underlying mechanism of the "electrostatic shielding effect" in aqueous Zn batteries. Adapted from refs. [104]. (**d**) The multifunctional inorganic additive $NH_4H_2PO_4$ promotes uniform deposition of zinc and inhibits side reactions. Reprinted from Ref. [106]. (**e**) Schematic of chaotropic anions regulating H-bond structure in bulk electrolyte. Reprinted from Ref. [107].

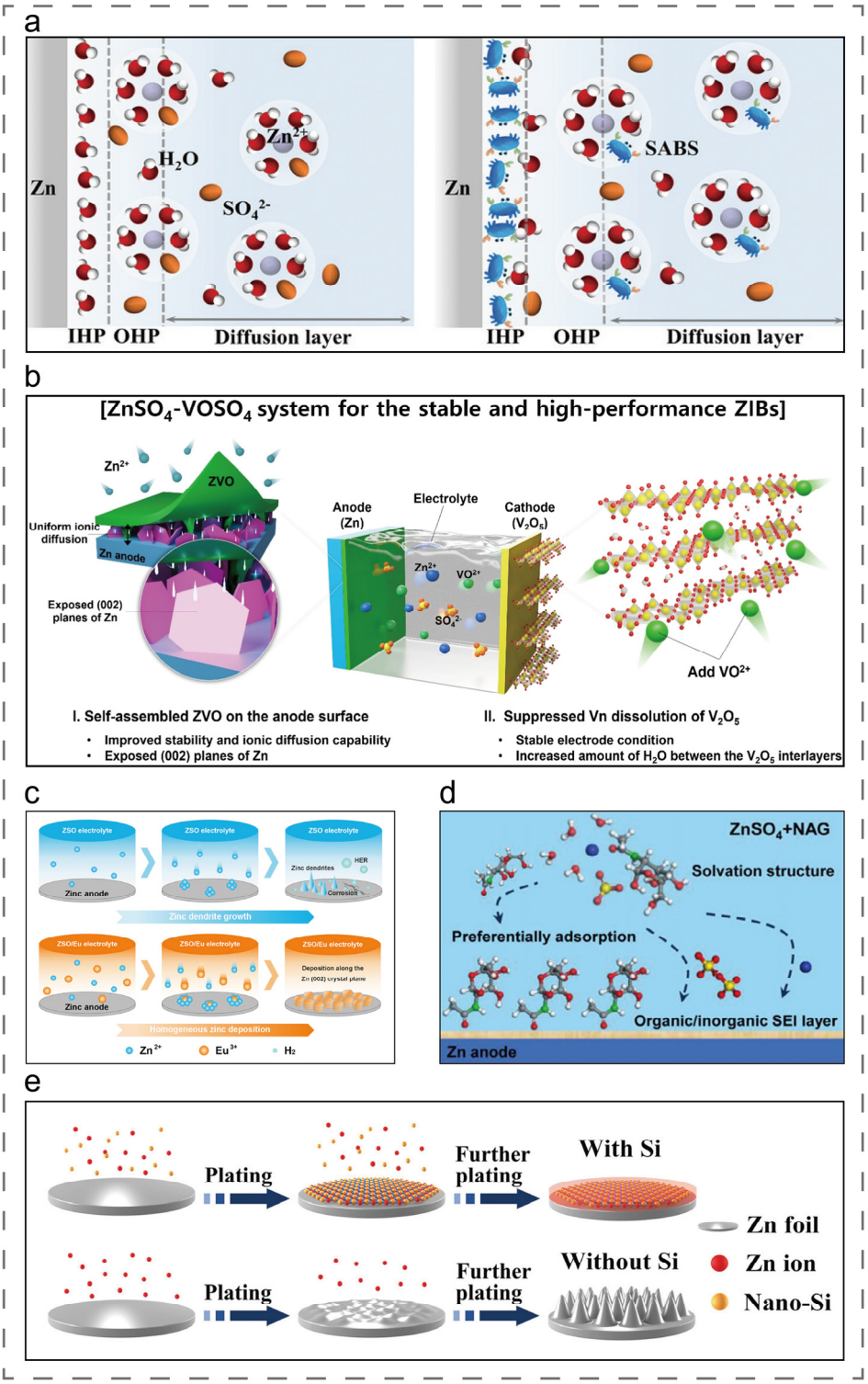


Figure 4. (**a**) Schematic diagram of EDL regulation. Reprinted with permission from ref. [112]. 2024, Wiley. (**b**) Schematic showing the advantages of the $ZnSO_4$-$VOSO_4$ system with the functional effects of the self-assembled passive layer on the anode surface and the inhibition of V dissolution at the cathode. Reprinted with permission from ref. [113]. 2023, Elsevier. (**c**) EuCl3 preferentially deposits zinc ions along the (002) crystal plane. Reprinted with permission from ref. [114]. 2024, Elsevier. (**d**) Schematic illustration of the reaction mechanism on the anode/electrolyte interface in $ZnSO_4$ + NAG. Reprinted with permission from ref. [115]. 2025, Wiley. (**e**) Schematic illustration of Zn plating process with nano-Si additive. Reprinted with permission from ref. [116]. 2023, Wiley.

In addition to the in-situ reduction of organic molecules, the introduction of inorganic salt components serves as an effective route to regulate interfacial crystallization thermodynamics and cultivate inorganic mineralized phases. Yoo et al. [113] reported a bipolar synergistic modulation strategy using vanadium oxysulfate ($VOSO_4$) as an active electrolyte additive (Figure 4b). On the anode side, $VOSO_4$ induces the in-situ self-assembly of a dense protective barrier that guides zinc deposition along the thermodynamically stable Zn(002) plane, enhancing interfacial ion diffusion kinetics while suppressing corrosion and passivation. Concurrently, on the cathode side, the common-ion effect established by the introduced $VOSO_4$ suppresses the irreversible dissolution of vanadium from the V_2O_5 matrix, delivering a discharge capacity of 590 $mAh{\cdot}g^{-1}$ at 1 $A{\cdot}g^{-1}$. To further leverage the kinetic regulation potential of heavy metal cations, Zhang et al. [114] introduced europium chloride ($EuCl_3$), a rare-earth halide, as a dual-functional additive (Figure 4c). This rare-earth salt manifests texture-engineering capabilities that elevate the hydrogen evolution overpotential while precisely modifying Zn^{2+} crystallization thermodynamics. This forces zinc to arrange tightly along the highly corrosion-resistant Zn(002) plane, driving the symmetric cells to endure over 3000 h of dendrite-free stripping/plating under rigorous parameters of 5 $mA{\cdot}cm^{-2}$/2 $mAh{\cdot}cm^{-2}$.

Conventional sulfate anions (SO_4^{2-}), owing to their high chemical inertness, are generally unfavorable for direct participation in SEI construction. To circumvent this thermodynamic constraint, Zhou et al. [115] introduced N-acetyl-D-glucosamine (NAG), a green biomass molecule (Figure 4d). The adsorbed NAG molecules not only reshape the EDL microenvironment but also serve as an interfacial catalyst that lowers the reduction activation energy of adjacent SO_4^{2-} anions. This coordinated pathway drives the deep decomposition of sulfate species under mild operating regimes, in situ generating a rigid, highly Zn^{2+}-conductive inorganic phase enriched with zinc sulfide (ZnS) and zinc carbonate ($ZnCO_3$). Seamlessly integrating the mechanical rigidity and ionic transport of inorganic crystals with the flexibility of organic cushions, this fluorine-free hybrid SEI effectively isolates water aggression, enabling a lifespan exceeding 6500 h at 0.5 $mA{\cdot}cm^{-2}$ and providing an instructive reference for transitioning inorganic electrolyte chemistry toward sustainable, multi-dimensional hybridization.

Beyond soluble inorganic salts, extending modifier precursors from ionic species to three-dimensional solid-state inorganic nanoparticles—and further cross-linking them with organic matrices—constitutes another essential branch of inorganic interphase engineering. Wu et al. [116] reported a strategy utilizing silicon nanoparticles (nano-Si) to customize the interfacial electric field (Figure 4e). Due to ambient oxidation, the nano-Si particles are naturally enveloped in a pristine hydroxylated layer (Si-OH). Upon electrodeposition, these surface hydroxyl groups chemically cross-link with incoming Zn^{2+} ions to weave a continuous, three-dimensional inorganic Si-O-Zn skeletal network. This solid network homogenizes the spatial distribution of localized charges and electric field intensities, lowering the zinc nucleation barrier and yielding a 5-fold lifespan extension (over 1250 cycles at 5 $mA{\cdot}cm^{-2}$) compared to the bare system.

3.4. Mechanism Analysis and Research Progress of Polymer Additives

Polymer additives—encompassing hydrophilic polymers, hydrogels, and supramolecular macromolecules—exhibit distinct advantages in the interfacial regulation of aqueous zinc-ion batteries (AZIBs) owing to their long-chain topologies, abundant multi-site functional groups, and spatial confinement effects. The macromolecular networks not only effectively anchor free water molecules through hydrogen-bonded networks to lower their thermodynamic activity, but also capitalize on fixed-charge electric fields to homogenize interfacial ionic fluxes. Furthermore, the flexible backbones of polymers seamlessly accommodate

the substantial volume fluctuations encountered during zinc stripping/plating. This subsection systematically reviews the research progress of polymer additives in stabilizing phase interfaces from three dimensions: supramolecular spatial confinement, side-chain charge regulation, and in-situ integrated dynamic self-healing interphases [117–122].

At the supramolecular level, utilizing the multimodal coordination of macromolecules or the host–guest adsorption effects of spatially stereocyclic macrocycles represents a classical approach to shielding free water and inducing preferred crystallographic orientations. Zhao et al. [123] reported a structure–activity modification paradigm based on cyclodextrin (CDs, including α-, β- and γ-CD) supramolecular macrocycles (Figure 5a). Exploiting the unique cavity property of being "hydrophobic inside and hydrophilic outside," α-CD chemically adsorbs onto the zinc foil surface via its peripheral secondary hydroxyl groups, weaving a supramolecular shield that physically isolates water molecules from corrosion. Concurrently, its electron-rich, zinc-loving outer surface exhibits prominent nucleation-inducing activity that substantially lowers the activation energy barrier (E_a), enabling Zn||Cu asymmetric cells to deliver a high average coulombic efficiency (CE) of 99.90%. To advance single-ion conduction to a higher level, Sun et al. [124] reported the construction of a single zinc-ion conducting hydrogel (SIHE) utilizing a pseudo-polyrotaxane (PPR) supramolecular architecture with a topological "slide-ring" mechanism (Figure 5b). Distinct from conventional rigid covalent grafting of anions, which often immobilizes polyvalent Zn^{2+} via intense Coulombic forces, this strategy threads linear polyethylene glycol (PEO) into cyclic α-CD cavities followed by in-situ cross-linking. Capitalizing on the steric hindrance of the macrocycles and the topological sliding degrees of freedom of the long chains, the anions are mechanically confined within the interspaces between adjacent macrocycles. Meanwhile, the electron-rich hydroxyl groups densely distributed on the outer edges of the macrocycles construct an unbonded channel for zinc flux, achieving a high zinc-ion transference number of $t_{Zn^{2+}}$ = 0.923 and an ionic conductivity of 22.4 $mS \cdot cm^{-1}$, which empowers the configured Zn||V_2O_5 cell to stably withstand 3500 cycles at 5C.

Beyond spatial steric shielding, reshaping the EDL mass transfer mechanism via side-chain charge repulsion of polymer long chains constitutes another crucial direction for macromolecular modification. Lin et al. [125] addressed the mass transport lag of zinc ions caused by the intricate "jump transport" mechanism in conventional neutral polymer matrices (such as PAM) by developing a functional polymer (PAPTMA) suspended with strong cationic quaternary ammonium salt groups (-N+R_3) on the side chains (Figure 6a). Relying on the electrostatic repulsion of like charges, these fixed positive charges create facilitated pathways for Zn^{2+} within the gel network, pushing the zinc-ion transference number to $t_{Zn^{2+}}$ = 0.79. Concurrently, the network effectively confines bulk free water as interfacial bound water, thereby suppressing the phase passivation of the byproduct $Zn_4(OH)_6SO_4 \cdot 5H_2O$ and endowing flexible pouch batteries with outstanding mechanical fatigue resistance.

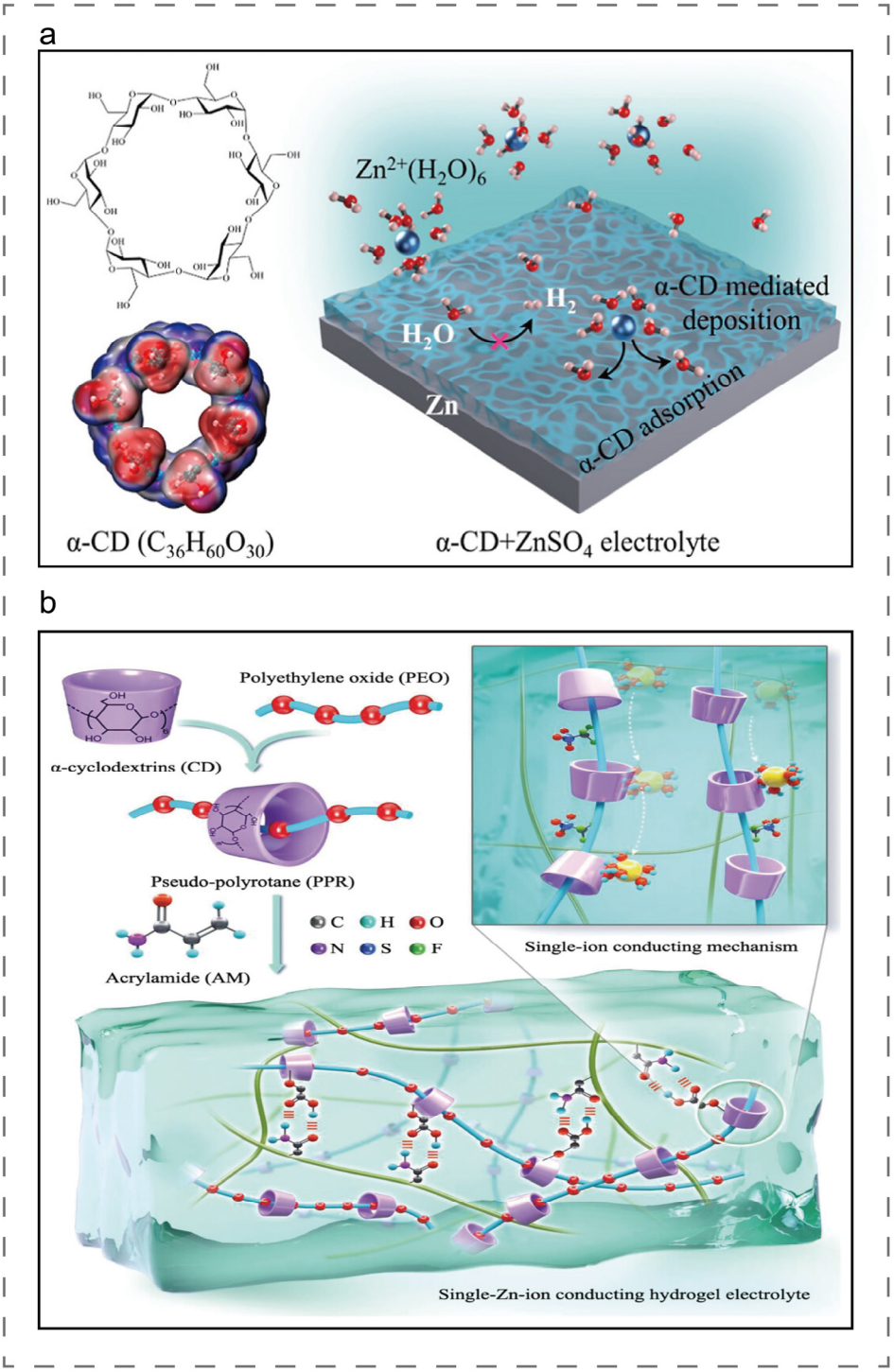


Figure 5. (**a**) Mechanism of CD molecules (α-, β-, and γ-CD) as electrolyte additives for rechargeable zinc batteries. Reprinted with permission from ref. [123]. 2022, American Chemical Society. (**b**) Schematic illustration of the fabrication process of CD-PEO/PAM hydrogel, where the anion can be physically confined between the two ring-shaped CDs and Zn^{2+} can be directed along the outside of the rings to form a single-Zn-ion conducting hydrogel electrolyte. Reprinted with permission from ref. [124]. 2023, Wiley.

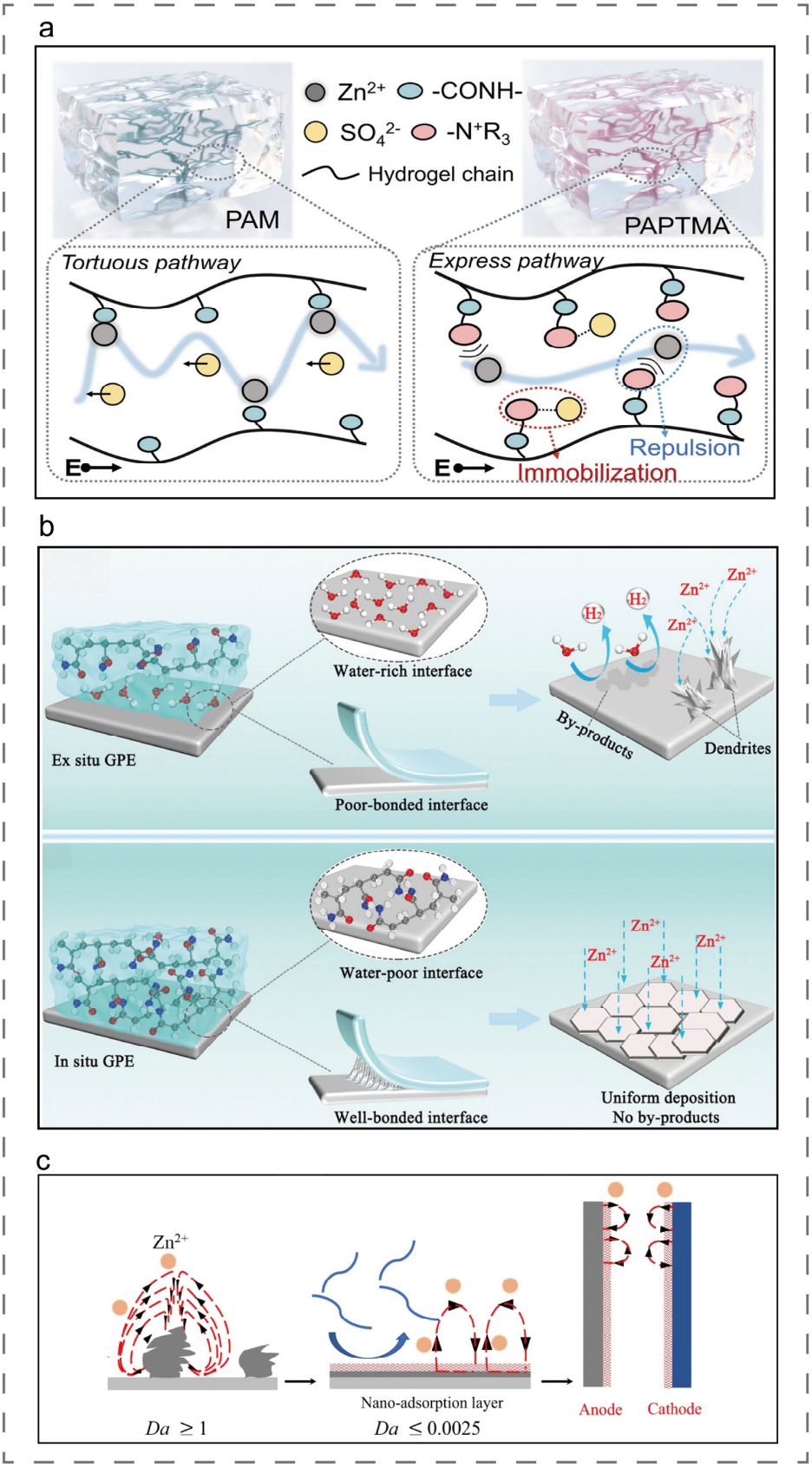


Figure 6. (**a**) Schematics of the ion transport within PAM and PAPTMA hydrogels. Reprinted from Ref. [125]. (**b**) Schematic of ex situ GPE and in situ GPE at the electrode–electrolyte interface. Reprinted with permission from ref. [126]. 2022 Wiley. (**c**) Ion movement mechanism in the cation-selective interval. Reprinted from Ref. [127].

The advanced evolution of polymer conditioning strategies lies in breaking the limitations of static physical contact imposed by conventional pre-made gels, moving toward in-situ cross-linking integration and "intelligently responsive phase interphases" with self-healing attributes. To circumvent the poor solid–solid interfacial contact, elevated impedance, and severe side reactions typical of external gel electrolytes, Qin et al. [126] proposed a "chemical welding" integration strategy that leverages the reducing capability of zinc foil to trigger in-situ redox polymerization (Figure 6b). The macromolecular precursor fluid spontaneously penetrates the microcracks on the zinc anode surface and, under the autocatalytic dissolution and chemical initiation of the zinc foil, directly solidifies and cross-links at the phase boundary to construct a seamless, continuous interphase. This not only eliminates contact resistance but also establishes a water-deficient microenvironment via macromolecular water-locking, driving symmetric cells to operate stably for over 240 h under demanding conditions of 40 $mA \cdot cm^{-2}$/40 $mAh \cdot cm^{-2}$ (DOD = 87%). On this basis, to overcome the practical challenge of rapid additive depletion under ultra-fast charging regimes, Jin et al. [127] utilized the interfacial adsorption behavior of oligomer-ion complexes to construct a responsive dynamic protective phase with a nanometer thickness in situ (Figure 6c). As verified by quartz crystal microbalance (QCM) measurements, a delicate "solid–liquid dynamic equilibrium" is maintained between the nanofilm and the oligomers dissolved in the bulk phase, conferring excellent self-healing traits to the phase interface. This oligomer boundary layer synergistically suppresses self-corrosion, dendrite protrusions, and hydrodynamic convective disturbances (such as the Marangoni effect), lowering the desolvation activation energy. This allows the zinc anode to sustain dendrite-free deposition even under an ultra-fast charging current density of 160 $mA \cdot cm^{-2}$ approaching the theoretical diffusion limit. Furthermore, it delivers a high energy density of 151 $Wh \cdot kg^{-1}$ and over 12,000 high-power cycles in a practical, large-area 9 cm^2 Zn||I_2 pouch cell.

4. Summary and Outlook

4.1. Summary

In conclusion, formulating electrolyte additives represents a practical and scalable approach to modulate Zn^{2+} solvation chemistry and optimize interface compatibility in $ZnSO_4$-based batteries [128–132]. Based on the mechanistic framework established in this review, recent advances have successfully transitioned from empirical trial and error toward targeted physical chemistry regulation [133–136]. Table 1 lists some key evaluations of representative electrolyte additive strategies. Additive strategies generally achieve their protective effects through three primary pathways: (1) disrupting the hydrogen-bonded network of bulk water and reforming the primary/secondary Zn^{2+} solvation sheaths to decrease desolvation barriers; (2) restructuring the electric double layer (EDL) via selective adsorption or electrostatic shielding to guide zinc deposition along thermodynamics-stable facets; and (3) inducing sacrificial reduction or chemical mineralization to construct rigid–flexible hybrid solid electrolyte interphases (SEIs). While these strategies have extended the lifespan of zinc anodes under specialized testing conditions, significant kinetic and engineering gaps remain before achieving viable technology deployment [137–143].

Table 1. Critical evaluation of representative electrolyte additive strategies based on their physical chemistry mechanisms, regulatory effects, and practical limitations.

Additive Category & Example	Typical Concentration	Primary Regulatory Mechanism	Impact on Zn^{2+} Solvation/EDL	HER Suppression & Morphology	Performance Under Realistic Conditions	Critical Practical Limitations
Sacrificial Additives (e.g., *SABS*)	Low (e.g., 1–10 mM)	Cathodic reduction governed by low LUMO energy level	Generates water-poor inner Helmholtz plane (IHP); induces in-situ SEI	Significant HER suppression; uniform layer-by-layer deposition	Generally evaluated under flooded cells; rapid depletion under lean electrolyte (E/C < 3 g·Ah^{-1})	Irreversible Consumption: Additive depletes over long-term deep cycling, requiring continuous replenishment.
Non-Sacrificial Surfactants (e.g., *SDBS*)	Low (e.g., 1 –5 mM)	Coordination chemistry governed by high HOMO energy level	Expels reactive H_2O from primary solvation sheath; chemisorption	Elevates HER overpotential; compact and smooth Zn surface	Moderate DOD (usually <30%); performance drops sharply at high current densities	Desorption under High Flux: Dynamic adsorption layer may fail or reorganize under extreme high-rate polarization.
Inorganic Modulators (e.g., $EuCl_3$)	Moderate (e.g., 0.1–0.5 M)	Inorganic mineralization and crystallographic guidance	Alters crystallization thermodynamics; induces preferential Zn(002) growth	Mechanical suppression of dendrites; highly textured deposits	Shows promise for deep discharge (DOD > 50%), but heavy ions increase mass	Cost & Transport: Rare-earth elements are expensive; large cations increase low-temperature mass-transfer resistance.
Cationic Shielding (e.g., Na^+, NH_4^+)	High (e.g., 0.5–2.0 M)	Electrostatic shielding at the dendrite tips	Accumulates at protrusions (sharp tips) without being reduced	Redirects Zn^{2+} flux to planar regions; delays short circuits	Heavily dependent on excess electrolyte; parasitic gas evolution persists over time	Insufficient Complete Protection: Fails to completely block free water attack; long-term water consumption still occurs.
Polymer Networks (e.g., *CHI*, *PEG*)	High (e.g., 1–5 wt%)	Steric confinement and bulk H-bond network disruption	Limits free water activity; constructs 3D single-ion transport channels	Acts as a physical barrier against water molecules; rounded Zn grains	Suppresses cross-talk at thick electrodes, but long-term mechanical stability is debated	Viscosity & Kinetics: Significantly increases electrolyte viscosity, reducing overall ionic conductivity and low-temperature kinetics.

4.2. Outlook

To guide future research toward rigorous development and practical implementation, the following key priorities must be addressed.

Decoupling Multi-Dimensional Descriptor Systems: Future additive screening should establish precise correlations between quantum chemical descriptors (LUMO vs. HOMO)

and real interfacial behaviors [144–146]. LUMO energy levels should strictly govern sacrificial reduction and SEI formation under cathodic polarization, whereas HOMO energy levels should rationalize non-sacrificial electrostatic adsorption and coordination chemistry. Incorporating machine learning and high-throughput computations can accelerate this rational design, provided models are validated by quantifiable experimental descriptors [147–150].

Advanced Diagnostics Under Non-Equilibrium Conditions: Most current evaluations rely heavily on static or post-test characterizations, which frequently obscure the transient dynamics at the phase boundary. Priority should be given to integrating operando techniques—such as liquid-phase transmission electron microscopy (LC-TEM), differential electrochemical mass spectrometry (DEMS), and cryo-TEM [151,152]. These tools are essential to monitor the real-time adsorption–desorption kinetics of additives under high current fluxes, capture chemical decomposition products at mild potentials, and identify transient failure modes of the boundary layers [153–155].

Validation Under Stringent, Industry-Relevant Parameters: The outstanding lifespans frequently reported in literature are predominantly achieved under idealized configurations (excessive electrolyte, thick zinc foils, and low areal capacities), which heavily mask realistic cell degradation. Future work must rigorously evaluate additives under standard industrial red lines: ultra-thin zinc anodes (<50 mum), high-mass-loading cathodes (>20 mg·cm^{-2}), high depths of discharge (DOD > 70%), and extremely lean electrolyte criteria [156,157]. Under these water-scarce regimes, understanding the continuous consumption rates of additives, their mechanical shear resistance against continuous volume changes, and their oxidation stability at high positive potentials is paramount for translating laboratory electrolyte chemistry into reliable energy storage systems.

Author Contributions: B.W.: Writing—original draft, Data curation, Visualization, Writing—review and editing. Y.R.: Writing—review and editing, Funding acquisition, Resources, Supervision. All authors have read and agreed to the published version of the manuscript.

Funding: This work was supported by the Yunnan Provincial Major Science and Technology Special Project (No. 202502AB080003), the Yunnan Xingdian Talent Support Plan-Talent Special Project (No. KKXX202452003) and the Program for Overseas High-Level Talents Returning to China (No. 109720240016).

Data Availability Statement: No data was used for the research described in the article.

Conflicts of Interest: The authors declare no conflicts of interest. The funders had no role in the design of the study; in the collection, analyses, or interpretation of data; in the writing of the manuscript; or in the decision to publish the results.

References

1. Zhao, Q.; Wang, Y.; Liu, W.; Liu, X.; Wang, H.; Yu, H.; Chen, Y.; Chen, L. An In-Depth Study of Regulable Zincophilic Alloy Matrix toward Stable Zinc Metal Batteries. *Adv. Mater. Interfaces* **2022**, *9*, 2102254. [CrossRef]
2. Lu, C.; Yang, Z.; Ding, Y.; Wang, Y.; Wang, X.; Li, T.; Tan, Q. Enhanced Electrochemical Performance of Ammonium Vanadate (NH4V4O10) Cathode for Rechargeable Aqueous Zinc-Ion Batteries by Altering pH Regulators. *Mater. Today Commun.* **2023**, *35*, 105993. [CrossRef]
3. Dai, Y.; Lu, R.; Zhang, C.; Li, J.; Yuan, Y.; Mao, Y.; Ye, C.; Cai, Z.; Zhu, J.; Li, J.; et al. Zn^{2+}-Mediated Catalysis for Fast-Charging Aqueous Zn-Ion Batteries. *Nat. Catal.* **2024**, *7*, 776–784. [CrossRef]
4. Chen, X.; Zhang, H.; Gao, Y.; Liu, J.; Cao, X.; Zhan, C.; Wang, S.; Wang, J.; Dou, S.; Cao, D. Zinc-ion Hybrid Supercapacitors: Design Strategies, Challenges, and Perspectives. *Carbon. Neutraliz.* **2022**, *1*, 159–188. [CrossRef]
5. Brown, J.; Aguilar, I.; Forero-Saboya, J.; Bihari Soni, C.; Chotard, H.; Wang, Y.; Zuras, E.; Noël, J.-M.; Tarascon, J.-M.; Grimaud, A. Zinc-Oligoether Carboxylate Salts as Electrolyte Additives for Aqueous Zn Metal Batteries. *Nat. Commun.* **2025**, *17*, 750. [CrossRef] [PubMed]
6. Song, T.-B.; Ma, Q.-L.; Zhang, X.-R.; Ni, J.-W.; He, T.-L.; Xiong, H.-M. Zn Anode Surface Engineering for Stable Zinc-Ion Batteries: Carbon Dots Incorporated Mesoporous TiO_2 as a Coating Layer. *Chem. Eng. J.* **2023**, *471*, 144735. [CrossRef]

7. Liu, X.; Yang, F.; Xu, W.; Zeng, Y.; He, J.; Lu, X. Zeolitic Imidazolate Frameworks as Zn^{2+} Modulation Layers to Enable Dendrite-Free Zn Anodes. *Adv. Sci.* **2020**, *7*, 2002173. [CrossRef] [PubMed]
8. Wang, L.; Liu, H.K.; Dou, S.X.; Huang, W.; Chong, S. Zinc Anode Stabilization in Aqueous Zinc-Ion Batteries: A Comprehensive Review of Challenges and Strategies. *Adv. Energy Mater.* **2026**, *16*, e70916. [CrossRef]
9. Schon, T.B.; McAllister, B.T.; Li, P.-F.; Seferos, D.S. The Rise of Organic Electrode Materials for Energy Storage. *Chem. Soc. Rev.* **2016**, *45*, 6345–6404. [CrossRef] [PubMed]
10. Zhang, Q.; Luan, J.; Tang, Y.; Ji, X.; Wang, H. Interfacial Design of Dendrite-Free Zinc Anodes for Aqueous Zinc-Ion Batteries. *Angew. Chem. Int. Ed.* **2020**, *59*, 13180–13191. [CrossRef] [PubMed]
11. Zhu, C.; Li, P.; Xu, G.; Cheng, H.; Gao, G. Recent Progress and Challenges of Zn Anode Modification Materials in Aqueous Zn-Ion Batteries. *Coord. Chem. Rev.* **2023**, *485*, 215142. [CrossRef]
12. Qian, X.; Li, L.; Wang, Y.; Tian, Z.; Zhong, H.; Chen, W.; Chen, T.; Fu, J. Versatile Metallo-Supramolecular Polymeric Interphase for Highly Reversible Zinc Metal Anodes. *Energy Storage Mater.* **2023**, *58*, 204–214. [CrossRef]
13. Du, W.; Ang, E.H.; Yang, Y.; Zhang, Y.; Ye, M.; Li, C.C. Challenges in the Material and Structural Design of Zinc Anode towards High-Performance Aqueous Zinc-Ion Batteries. *Energy Environ. Sci.* **2020**, *13*, 3330–3360. [CrossRef]
14. Dai, H.; Sun, T.; Zhou, J.; Wang, J.; Chen, Z.; Zhang, G.; Sun, S. Unraveling Chemical Origins of Dendrite Formation in Zinc-Ion Batteries via in Situ/Operando X-Ray Spectroscopy and Imaging. *Nat. Commun.* **2024**, *15*, 8577. [CrossRef] [PubMed]
15. Kim, H.J.; Kim, S.; Yu, J.H.; Lim, J.-H.; Yashiro, H.; Myung, S.-T. Unlocking Long-Term Stability: Electrolyte Additives for Suppressing Zinc Dendrite Growth in Aqueous Zinc Metal Batteries. *Chem. Eng. J.* **2025**, *506*, 160017. [CrossRef]
16. Liu, W.; Liu, P.; Mitlin, D. Tutorial Review on Structure–Dendrite Growth Relations in Metal Battery Anode Supports. *Chem. Soc. Rev.* **2020**, *49*, 7284–7300. [CrossRef] [PubMed]
17. Wei, J.; Zhang, P.; Sun, J.; Liu, Y.; Li, F.; Xu, H.; Ye, R.; Tie, Z.; Sun, L.; Jin, Z. Advanced Electrolytes for High-Performance Aqueous Zinc-Ion Batteries. *Chem. Soc. Rev.* **2024**, *53*, 10335–10369. [CrossRef] [PubMed]
18. Zhu, M.; Ku, S.; Ran, Q.; Huang, H.; Cao, N.; Bai, F.-Q.; Lang, X.-Y.; Chao, D.; Feng, M. Ion-Directed Polymer/Inorganic Interphase with Enriched Charge for Stable and High-Rate Zn Anodes. *Energy Environ. Sci.* **2026**, *19*, 3629–3639. [CrossRef]
19. Tian, H.; Feng, G.; Wang, Q.; Li, Z.; Zhang, W.; Lucero, M.; Feng, Z.; Wang, Z.-L.; Zhang, Y.; Zhen, C.; et al. Three-Dimensional Zn-Based Alloys for Dendrite-Free Aqueous Zn Battery in Dual-Cation Electrolytes. *Nat. Commun.* **2022**, *13*, 7922. [CrossRef] [PubMed]
20. Chang, Z.; Yang, H.; Qiao, Y.; Zhu, X.; He, P.; Zhou, H. Tailoring the Solvation Sheath of Cations by Constructing Electrode Front-Faces for Rechargeable Batteries. *Adv. Mater.* **2022**, *34*, e2201339. [CrossRef] [PubMed]
21. Cheng, X.; Dong, J.; Yang, H.; Li, X.; Zhao, X.; Chen, B.; Zhang, Y.; Liu, M.; Wang, J.; Lin, H. Tailoring Solvation Sheath for Rechargeable Zinc-Ion Batteries: Progress and Prospect. *Mater. Rep. Energy* **2025**, *5*, 100313. [CrossRef]
22. Yang, Y.; Liu, C.; Lv, Z.; Yang, H.; Zhang, Y.; Ye, M.; Chen, L.; Zhao, J.; Li, C.C. Synergistic Manipulation of Zn^{2+} Ion Flux and Desolvation Effect Enabled by Anodic Growth of a 3D ZnF_2 Matrix for Long-Lifespan and Dendrite-Free Zn Metal Anodes. *Adv. Mater.* **2021**, *33*, 2007388. [CrossRef] [PubMed]
23. Luo, J.; Xu, L.; Yang, Y.; Huang, S.; Zhou, Y.; Shao, Y.; Wang, T.; Tian, J.; Guo, S.; Zhao, J.; et al. Stable Zinc Anode Solid Electrolyte Interphase via Inner Helmholtz Plane Engineering. *Nat. Commun.* **2024**, *15*, 6471. [CrossRef] [PubMed]
24. Wan, Y.; Huang, L.; Bu, F.; Sun, Z.; Zhang, S.; Zhao, Z.; Li, L.; Chao, D.; Zhao, D.; Luo, W. Large-Pore Mesoporous Covalent Organic Frameworks as Fast Ion Sieves via Kinetics-Mediated Micelle Assembly for Aqueous Batteries. *Energy Environ. Sci.* **2026**, *19*, 3944–3955. [CrossRef]
25. Zeng, F.; Li, S.; Hu, S.; Qiu, M.; Zhang, G.; Li, M.; Chang, C.; Wang, H.; Xu, M.; Zheng, L.; et al. Weak Solvation Effect Enhancing Capacity and Rate Performance of Vanadium-Based Calcium Ion Batteries: A Strategy Guided by Donor Number. *Adv. Funct. Mater.* **2024**, *34*, 2302397. [CrossRef]
26. Peng, Z.; Li, S.; Tang, L.; Zheng, J.; Tan, L.; Chen, Y. Water-Shielding Electric Double Layer and Stable Interphase Engineering for Durable Aqueous Zinc-Ion Batteries. *Nat. Commun.* **2025**, *16*, 4490. [CrossRef] [PubMed]
27. Li, M.; Zhang, Y.; Hu, J.; Wang, X.; Zhu, J.; Niu, C.; Han, C.; Mai, L. Universal Multifunctional Hydrogen Bond Network Construction Strategy for Enhanced Aqueous Zn^{2+}/Proton Hybrid Batteries. *Nano Energy* **2022**, *100*, 107539. [CrossRef]
28. Tang, B.; Shan, L.; Liang, S.; Zhou, J. Issues and Opportunities Facing Aqueous Zinc-Ion Batteries. *Energy Environ. Sci.* **2019**, *12*, 3288–3304. [CrossRef]
29. Zhang, T.; Tang, Y.; Guo, S.; Cao, X.; Pan, A.; Fang, G.; Zhou, J.; Liang, S. Fundamentals and Perspectives in Developing Zinc-Ion Battery Electrolytes: A Comprehensive Review. *Energy Environ. Sci.* **2020**, *13*, 4625–4665. [CrossRef]
30. Pu, S.D.; Hu, B.; Li, Z.; Yuan, Y.; Gong, C.; Ning, Z.; Chau, C.; Yang, S.; Zhang, S.; Pi, L.; et al. Decoupling, Quantifying, and Restoring Aging-Induced Zn-Anode Losses in Rechargeable Aqueous Zinc Batteries. *Joule* **2023**, *7*, 366–379. [CrossRef]
31. Luo, H.; Gou, Q.; Zheng, Y.; Wang, K.; Yuan, R.; Zhang, S.; Fang, W.; Luogu, Z.; Hu, Y.; Mei, H.; et al. Machine Learning-Assisted High-Donor-Number Electrolyte Additive Screening toward Construction of Dendrite-Free Aqueous Zinc-Ion Batteries. *ACS Nano* **2025**, *19*, 2427–2443. [CrossRef] [PubMed]

32. Wei, T.; Zhang, H.; Ren, Y.; Mo, L.; He, Y.; Tan, P.; Huang, Y.; Li, Z.; Zhu, D.; Hu, L. Building Near-Unity Stacked (002) Texture for High-Stable Zinc Anode. *Adv. Funct. Mater.* **2024**, *34*, 2312506. [CrossRef]
33. Zhao, F.; Li, J.; Chutia, A.; Liu, L.; Kang, L.; Lai, F.; Dong, H.; Gao, X.; Tan, Y.; Liu, T.; et al. Highly Stable Manganese Oxide Cathode Material Enabled by Grotthuss Topochemistry for Aqueous Zinc Ion Batteries. *Energy Environ. Sci.* **2024**, *17*, 1497–1508. [CrossRef]
34. Zhang, L.; Ding, H.; Gao, H.; Gong, J.; Guo, H.; Zhang, S.; Yu, Y.; He, G.; Deng, T.; Parkin, I.P.; et al. An Integrated Design for High-Energy, Durable Zinc–Iodine Batteries with Ultra-High Recycling Efficiency. *Energy Environ. Sci.* **2025**, *18*, 2462–2473. [CrossRef]
35. Shang, Y.; Kundu, D. A Path Forward for the Translational Development of Aqueous Zinc-Ion Batteries. *Joule* **2023**, *7*, 244–250. [CrossRef]
36. Wu, B.; Yan, T.; Liu, S.; Su, Y.; Xiang, C.; Li, M.; Cui, Z.; Du, L.; Liang, Z.; Song, H. Reconstructing Electric Double Layer with β-Diketone Additive for Highly Invertible Zn Anode. *Adv. Funct. Mater.* **2025**, *35*, 2421244. [CrossRef]
37. Qian, X.; Chen, T.; Wang, Y.; Zhang, Q.; Li, W.; Fu, J. Revitalizing Dead Zinc with Ferrocene/Ferrocenium Redox Chemistry for Deep-Cycle Zinc Metal Batteries. *Angew. Chem. Int. Ed.* **2025**, *64*, e202412989. [CrossRef] [PubMed]
38. Zhou, Y.; Li, G.; Feng, S.; Qin, H.; Wang, Q.; Shen, F.; Liu, P.; Huang, Y.; He, H. Regulating Zn Ion Desolvation and Deposition Chemistry Toward Durable and Fast Rechargeable Zn Metal Batteries. *Adv. Sci.* **2023**, *10*, 2205874. [CrossRef] [PubMed]
39. Han, Y.; Xu, N.; Yin, Y.; Ruan, Z.; Shen, Y.; Fang, S.; Yang, L. Recent Advances in Stabilization Strategies for Zinc Anodes in Aqueous Zinc-Ion Batteries. *Front. Energy* **2025**, *19*, 862–883. [CrossRef]
40. Fang, G.; Zhou, J.; Pan, A.; Liang, S. Recent Advances in Aqueous Zinc-Ion Batteries. *ACS Energy Lett.* **2018**, *3*, 2480–2501. [CrossRef]
41. Wang, S.; Yang, D.; Zhang, P.; Guo, Y.; Liu, X.; Zhao, M.; Zhu, J.; Li, P.; Li, X.; Fan, J.; et al. Liquid Metal Anode Enables Zinc-Based Flow Batteries with Ultrahigh Areal Capacity and Ultralong Duration. *Sci. Adv.* **2025**, *11*, eads3919. [CrossRef] [PubMed]
42. Zhi, J.; Zhao, S.; Zhou, M.; Wang, R.; Huang, F. A Zinc-Conducting Chalcogenide Electrolyte. *Sci. Adv.* **2023**, *9*, eade2217. [CrossRef] [PubMed]
43. Li, C.; Wang, T.; Lai, H.C.J.; Park, S.W.; Chan, W.Y.K.; Li, Q.; Zhao, Y.; Fan, J.; Pei, Z.; Zhi, C. Hydrophobic-Unit-Regulated Hydrogel Electrolytes with High Water Content and Low Salt Concentration for High-Voltage Aqueous Batteries. *Joule* **2025**, *9*, 101827. [CrossRef]
44. Cai, Y.; Zhang, H.; Wang, T.; Xi, S.; Song, Y.; Rong, S.; Ma, J.; Han, Z.; Low, C.T.J.; Wang, Q.; et al. Directional Regulation on Single-Molecule Redox-Targeting Reaction in Neutral Zinc-Iron Flow Batteries. *Joule* **2025**, *9*, 101768. [CrossRef]
45. Tong, Z.; Wang, W.; Zeng, S.; Sun, Y.; Meng, J.; Liu, Y.; Xia, Q.; Yu, H. Hydrogen Bond Reconstruction Strategy for Eutectic Solvents That Realizes Room-Temperature Dissolution of Cellulose. *Green. Chem.* **2022**, *24*, 8760–8769. [CrossRef]
46. Li, Y.; Wang, Z.; Cai, Y.; Pam, M.E.; Yang, Y.; Zhang, D.; Wang, Y.; Huang, S. Designing Advanced Aqueous Zinc-Ion Batteries: Principles, Strategies, and Perspectives. *Energy Env. Mater.* **2022**, *5*, 823–851. [CrossRef]
47. Gourley, S.W.D.; Brown, R.; Adams, B.D.; Higgins, D. Zinc-Ion Batteries for Stationary Energy Storage. *Joule* **2023**, *7*, 1415–1436. [CrossRef]
48. Li, Y.-M.; Li, W.-H.; Li, K.; Jiang, W.-B.; Tang, Y.-Z.; Zhang, X.-Y.; Yuan, H.-Y.; Zhang, J.-P.; Wu, X.-L. Molecular Synergistic Effects Mediate Efficient Interfacial Chemistry: Enabling Dendrite-Free Zinc Anode for Aqueous Zinc-Ion Batteries. *J. Am. Chem. Soc.* **2024**, *146*, 30998–31011. [CrossRef] [PubMed]
49. Qin, T.; Li, K.; Liu, Y.; Xu, Z.; Gao, C. Low-Concentration Hydrogel Polyelectrolyte with In Situ Formed Interphases Enables 2.7 V Aqueous Pouch Cell. *Adv. Energy Mater.* **2023**, *13*, 2300733. [CrossRef]
50. Fu, B.; Liu, G.; Zhang, Y.; Liu, Z.; Xie, X.; Fang, G.; Liang, S. Zn Powder-Based Anodes for Aqueous Zn Metal Batteries: Strategies, Structures, and Perspectives. *ACS Energy Lett.* **2024**, *9*, 3292–3307. [CrossRef]
51. Jin, S.; Shao, Y.; Gao, X.; Chen, P.; Zheng, J.; Hong, S.; Yin, J.; Joo, Y.L.; Archer, L.A. Designing Interphases for Practical Aqueous Zinc Flow Batteries with High Power Density and High Areal Capacity. *Sci. Adv.* **2022**, *8*, eabq4456. [CrossRef] [PubMed]
52. Shin, C.; Yao, L.; Jeong, S.-Y.; Ng, T.N. Zinc-Copper Dual-Ion Electrolytes to Suppress Dendritic Growth and Increase Anode Utilization in Zinc Ion Capacitors. *Sci. Adv.* **2024**, *10*, eadf9951. [CrossRef] [PubMed]
53. Gao, X.; Dai, Y.; Zhang, C.; Zhang, Y.; Zong, W.; Zhang, W.; Chen, R.; Zhu, J.; Hu, X.; Wang, M.; et al. When It's Heavier: Interfacial and Solvation Chemistry of Isotopes in Aqueous Electrolytes for Zn-ion Batteries. *Angew. Chem.* **2023**, *135*, e202300608. [CrossRef]
54. Cao, X.; Xu, W.; Zheng, D.; Wang, F.; Wang, Y.; Shi, X.; Lu, X. Weak Solvation Effect Induced Optimal Interfacial Chemistry Enables Highly Durable Zn Anodes for Aqueous Zn-Ion Batteries. *Angew. Chem. Int. Ed.* **2024**, *63*, e202317302. [CrossRef] [PubMed]
55. Chen, Y.; Zhao, Q.; Liu, W.; Chen, L. Ultra-Stable Zn Metal Batteries with Dendrite-Free Cu-Sn Alloy Induced High-Quality Composite Zn Mesh. *SSRN J.* **2022**, *450*, 137979. [CrossRef]

56. Tong, Y.; Zang, Y.; Su, S.; Zhang, Y.; Fang, J.; Yang, Y.; Li, X.; Wu, X.; Chen, F.; Hou, J.; et al. Methylene Blue Intercalated Vanadium Oxide with Synergistic Energy Storage Mechanism for Highly Efficient Aqueous Zinc Ion Batteries. *J. Energy Chem.* **2023**, *77*, 269–279. [CrossRef]
57. Deng, S.; Yan, X.; Jiang, Y.; Li, A.; Zhang, R.; Qu, Y.; Xie, Z. Hydrophobic Interface Induced by Fluorine Doping Enhances Vanadium Oxide Cathodes for Aqueous Zinc-Ion Batteries. *Chem. Eng. J.* **2025**, *503*, 158472. [CrossRef]
58. Yang, S.; Mei, L.; Wu, Z.; Zhu, J.; Li, P.; Hong, H.; Zeng, Z.; Li, H.; Mo, F.; Zhi, C. Overcharge Protection in Aqueous Zinc-Ion Batteries via Self-Sacrificial Additives. *Energy Environ. Sci.* **2024**, *17*, 7424–7434. [CrossRef]
59. Liu, C.; Neale, Z.; Zheng, J.; Jia, X.; Huang, J.; Yan, M.; Tian, M.; Wang, M.; Yang, J.; Cao, G. Expanded Hydrated Vanadate for High-Performance Aqueous Zinc-Ion Batteries. *Energy Environ. Sci.* **2019**, *12*, 2273–2285. [CrossRef]
60. Li, Q.; Chen, A.; Wang, D.; Zhao, Y.; Wang, X.; Jin, X.; Xiong, B.; Zhi, C. Tailoring the Metal Electrode Morphology via Electrochemical Protocol Optimization for Long-Lasting Aqueous Zinc Batteries. *Nat. Commun.* **2022**, *13*, 3699. [CrossRef] [PubMed]
61. Hao, J.; Yuan, L.; Zhu, Y.; Jaroniec, M.; Qiao, S. Triple-Function Electrolyte Regulation toward Advanced Aqueous Zn-Ion Batteries. *Adv. Mater.* **2022**, *34*, 2206963. [CrossRef] [PubMed]
62. Geng, L.; Meng, J.; Wang, X.; Wu, W.; Han, K.; Huang, M.; Han, C.; Wu, L.; Li, J.; Zhou, L.; et al. Organic-Solvent-Free Primary Solvation Shell for Low-Temperature Aqueous Zinc Batteries. *Chem* **2025**, *11*, 102302. [CrossRef]
63. Chu, S.; Majumdar, A. Opportunities and Challenges for a Sustainable Energy Future. *Nature* **2012**, *488*, 294–303. [CrossRef]
64. Arjona, N.; Álvarez Contreras, L.; Guerra Balcázar, M. (Eds.) *Surface and Interfacial Defects in Nanomaterials for Sustainable Energy Production and Storage*; Wiley-VCH: Weinheim, Germany, 2026; ISBN 978-3-527-35464-1.
65. Huang, Z.; Zhou, G.; Lv, W.; Deng, Y.; Zhang, Y.; Zhang, C.; Kang, F.; Yang, Q.-H. Seeding Lithium Seeds towards Uniform Lithium Deposition for Stable Lithium Metal Anodes. *Nano Energy* **2019**, *61*, 47–53. [CrossRef]
66. Meng, Y.; Wang, M.; Wang, J.; Huang, X.; Zhou, X.; Sajid, M.; Xie, Z.; Luo, R.; Zhu, Z.; Zhang, Z.; et al. Robust Bilayer Solid Electrolyte Interphase for Zn Electrode with High Utilization and Efficiency. *Nat. Commun.* **2024**, *15*, 8431. [CrossRef] [PubMed]
67. Xie, C.; Wang, C.; Xu, Y.; Li, T.; Fu, Q.; Li, X. Reversible Multielectron Transfer I−/IO3− Cathode Enabled by a Hetero-Halogen Electrolyte for High-Energy-Density Aqueous Batteries. *Nat. Energy* **2024**, *9*, 714–724. [CrossRef]
68. Ma, L.; Schroeder, M.A.; Borodin, O.; Pollard, T.P.; Ding, M.S.; Wang, C.; Xu, K. Realizing High Zinc Reversibility in Rechargeable Batteries. *Nat. Energy* **2020**, *5*, 743–749. [CrossRef]
69. Yuan, Z.; Liang, L.; Dai, Q.; Li, T.; Song, Q.; Zhang, H.; Hou, G.; Li, X. Low-Cost Hydrocarbon Membrane Enables Commercial-Scale Flow Batteries for Long-Duration Energy Storage. *Joule* **2022**, *6*, 884–905. [CrossRef]
70. Dai, Y.; Zhang, C.; Zhang, X.; Jiang, P.; Chen, J.; Zong, W.; Zheng, S.; Gao, X.; Macdonald, T.J.; He, G. Interfacial Energy Storage in Aqueous Zinc-Ion Batteries. *Energy Environ. Sci.* **2025**, *18*, 9018–9030. [CrossRef]
71. Shi, Z.; Chen, S.; Xu, Z.; Liu, Z.; Guo, J.; Yin, J.; Xu, P.; Zhang, N.; Zhang, W.; Alshareef, H.N.; et al. Metal Oxide Aerogels: A New Horizon for Stabilizing Anodes in Rechargeable Zinc Metal Batteries. *Adv. Energy Mater.* **2023**, *13*, 2300331. [CrossRef]
72. Zhao, Q.; Huang, W.; Luo, Z.; Liu, L.; Lu, Y.; Li, Y.; Li, L.; Hu, J.; Ma, H.; Chen, J. High-Capacity Aqueous Zinc Batteries Using Sustainable Quinone Electrodes. *Sci. Adv.* **2018**, *4*, eaao1761. [CrossRef] [PubMed]
73. Feng, Z.; Feng, Y.; Fan, F.; Deng, D.; Dong, H.; Liu, S.; Kang, L.; Jun, S.C.; Wang, L.; Zhu, J.; et al. Functionalization Design of Zinc Anode for Advanced Aqueous Zinc-ion Batteries. *SusMat* **2024**, *4*, e184. [CrossRef]
74. Zhang, Q.-K.; Zhang, X.-Q.; Wan, J.; Yao, N.; Song, T.-L.; Xie, J.; Hou, L.-P.; Zhou, M.-Y.; Chen, X.; Li, B.-Q.; et al. Homogeneous and Mechanically Stable Solid–Electrolyte Interphase Enabled by Trioxane-Modulated Electrolytes for Lithium Metal Batteries. *Nat. Energy* **2023**, *8*, 725–735. [CrossRef]
75. Gan, H.; Li, H.; Xu, M.; Han, C.; Cheng, H.-M. Failure Mechanisms and Remedy of an Ultrathin Zn Metal Anode in Pouch Cells. *Joule* **2024**, *8*, 3054–3071. [CrossRef]
76. Guo, H.; Shao, Z.; Zhang, Y.; Cui, X.; Mao, L.; Cheng, S.; Ma, M.; Lan, W.; Su, Q.; Xie, E. Electrolyte Additives Inhibit the Surface Reaction of Aqueous Sodium/Zinc Battery. *J. Colloid. Interface Sci.* **2022**, *608*, 1481–1488. [CrossRef] [PubMed]
77. Li, T.; Dong, X.; Yang, H.; Zhang, J.; Huang, R.; Lv, Z.; Li, Y.; Zhang, S.; Huang, F.; Lin, T. Defective 1T-VS_2 with Fibonacci Pattern Unlocking High Mass-Loading and Self-Charging Cathodes for Aqueous Zinc-Ion Batteries. *Energy Environ. Sci.* **2025**, *18*, 3169–3176. [CrossRef]
78. Zheng, X.; Liu, Z.; Sun, J.; Luo, R.; Xu, K.; Si, M.; Kang, J.; Yuan, Y.; Liu, S.; Ahmad, T.; et al. Constructing Robust Heterostructured Interface for Anode-Free Zinc Batteries with Ultrahigh Capacities. *Nat. Commun.* **2023**, *14*, 76. [CrossRef] [PubMed]
79. Liang, Y.; Yao, Y. Designing Modern Aqueous Batteries. *Nat. Rev. Mater.* **2022**, *8*, 109–122. [CrossRef]
80. Zhang, B.; Fan, H.J. Overlooked Calendar Issues of Aqueous Zinc Metal Batteries. *Joule* **2025**, *9*, 101802. [CrossRef]
81. Yan, H.; Li, S.; Zhong, J.; Li, B. An Electrochemical Perspective of Aqueous Zinc Metal Anode. *Nano-Micro Lett.* **2024**, *16*, 15. [CrossRef] [PubMed]
82. Yang, C.; Xia, J.; Cui, C.; Pollard, T.P.; Vatamanu, J.; Faraone, A.; Dura, J.A.; Tyagi, M.; Kattan, A.; Thimsen, E.; et al. All-Temperature Zinc Batteries with High-Entropy Aqueous Electrolyte. *Nat. Sustain.* **2023**, *6*, 325–335. [CrossRef]

83. Qu, Y.; Qian, J.; Zhang, F.; Zhu, Z.; Zhu, Y.; Hou, Z.; Meng, Q.; Chen, K.; Dou, S.X.; Chen, L. Constructing 3D Crosslinked Macromolecular Networks as a Highly Efficient Interface Layer for Ultra-Stable Zn Metal Anodes. *Adv. Mater.* **2025**, *37*, 2413370. [CrossRef] [PubMed]
84. Liu, J.; Xu, C.; Chen, Z.; Ni, S.; Shen, Z.X. Progress in Aqueous Rechargeable Batteries. *Green. Energy Environ.* **2018**, *3*, 20–41. [CrossRef]
85. Jiang, H.; Tang, L.; Fu, Y.; Wang, S.; Sandstrom, S.K.; Scida, A.M.; Li, G.; Hoang, D.; Hong, J.J.; Chiu, N.-C.; et al. Chloride Electrolyte Enabled Practical Zinc Metal Battery with a Near-Unity Coulombic Efficiency. *Nat. Sustain.* **2023**, *6*, 806–815. [CrossRef]
86. Parker, J.F.; Ko, J.S.; Rolison, D.R.; Long, J.W. Translating Materials-Level Performance into Device-Relevant Metrics for Zinc-Based Batteries. *Joule* **2018**, *2*, 2519–2527. [CrossRef]
87. Larcher, D.; Tarascon, J.-M. Towards Greener and More Sustainable Batteries for Electrical Energy Storage. *Nat. Chem.* **2015**, *7*, 19–29. [CrossRef] [PubMed]
88. Wang, Y.; Zhao, R.; Liu, M.; Yang, J.; Zhang, A.; Yue, J.; Wu, C.; Bai, Y. Suppressed Water Reactivity by Zincophilic-Hydrophobic Electrolyte Additive for Superior Aqueous Zn Metal Batteries. *Adv. Energy Mater.* **2023**, *13*, 2302707. [CrossRef]
89. Zhai, Y.; Xie, B.; Zheng, C.; Lang, H.; Li, L.; Yang, Y.; Luo, Y.; Tan, X.; Zheng, Q.; Lam, K.-H.; et al. Trace Alcohol Ether Electrolytes with Dual-Site Hydrogen Bonds and Modulated Solvation Structures for Ultralong-Life Zinc-Ion Batteries. *J. Colloid. Interface Sci.* **2025**, *678*, 886–895. [CrossRef] [PubMed]
90. Wei, T.; Mo, L.; Ren, Y.; Zhang, H.; Wang, M.; He, Y.; Tan, P.; Li, Z.; Chen, W.; Hu, L. Non-Sacrificial Anionic Surfactant with High HOMO Energy Level as a General Descriptor for Zinc Anode. *Energy Storage Mater.* **2024**, *70*, 103525. [CrossRef]
91. Zhang, Q.; Ma, Y.; Lu, Y.; Zhou, X.; Lin, L.; Li, L.; Yan, Z.; Zhao, Q.; Zhang, K.; Chen, J. Designing Anion-Type Water-Free Zn^{2+} Solvation Structure for Robust Zn Metal Anode. *Angew. Chem. Int. Ed.* **2021**, *60*, 23357–23364. [CrossRef] [PubMed]
92. Shi, Z.; Li, M.; Fu, X.; Zhang, Y.; Jiao, S.; Zhao, Y. Bimodal Block Molecule with Ether-Type and Hydroxyl-Type Oxygen Stabilizes Zn Anode in Super-Dilute Electrolyte. *Adv. Funct. Mater.* **2024**, *34*, 2316427. [CrossRef]
93. Dong, D.; Heo, J.; Li, Z.; Zhang, Q.; Zhang, X.; Xia, K.; Niu, Y.; Wang, Z.; Hu, E.; Wang, C. Aqueous Electrolyte Solutions with Anion-Bridged Secondary Solvation Sheaths for Highly Efficient Zinc Metal Batteries. *Nat. Nanotechnol.* **2026**, *21*, 699–708. [CrossRef] [PubMed]
94. Yu, Y.; Zhang, P.; Wang, W.; Liu, J. Tuning the Electrode/Electrolyte Interface Enabled by a Trifunctional Inorganic Oligomer Electrolyte Additive for Highly Stable and High-Rate Zn Anodes. *Small Methods* **2023**, *7*, 2300546. [CrossRef] [PubMed]
95. Rajagopalan, R.; Tang, Y.; Jia, C.; Ji, X.; Wang, H. Understanding the Sodium Storage Mechanisms of Organic Electrodes in Sodium Ion Batteries: Issues and Solutions. *Energy Environ. Sci.* **2020**, *13*, 1568–1592. [CrossRef]
96. Kittner, N.; Lill, F.; Kammen, D.M. Energy Storage Deployment and Innovation for the Clean Energy Transition. *Nat. Energy* **2017**, *2*, 17125. [CrossRef]
97. Nithya, C.; Lakshmi, R.; Gopukumar, S. Effect of Mg Dopant on the Electrochemical Performance of $LiNi_{0.5}$ $Mn_{0.5}$ O_2 Cathode Materials for Lithium Rechargeable Batteries. *J. Electrochem. Soc.* **2012**, *159*, A1335–A1340. [CrossRef]
98. Zhong, W.; Cheng, H.; Zhang, S.; Li, L.; Tan, C.; Chen, W.; Lu, Y. Cation-Driven Phase Transition and Anion-Enhanced Kinetics for High Energy Efficiency Zinc-Interhalide Complex Batteries. *Nat. Commun.* **2025**, *16*, 4586. [CrossRef] [PubMed]
99. Zhang, Z.; Mu, Y.; Xiao, L.; Hu, H.; Xue, T.; Zang, L.; Sakai, E.; Han, M.; Yang, C.; Zeng, L.; et al. Hydrogel Electrolytes for Zinc-Ion Batteries: Materials Design, Functional Strategies, and Future Perspectives. *Nano-Micro Lett.* **2026**, *18*, 139. [CrossRef] [PubMed]
100. Lin, Z.; Zhang, Y.; Lin, X.; Ding, H.; Ye, M.; Wen, Z.; Tang, Y.; Liu, X.; Li, C.C. Reinforcing an Interfacial Molecular Dam through a Multifunctional Organic Electrolyte Additive for Stable Zn Anodes. *J. Mater. Chem. A* **2024**, *12*, 24226–24236. [CrossRef]
101. Wang, Y.; Zhao, R.; Yang, J.; Zou, J.; Zhang, A.; Han, X.; Hu, Z.; Lv, M.; Wang, X.; Wu, C.; et al. Toward the Rechargeable Aqueous Zinc Ion Batteries with Improved Overall Performance: Electrolyte with Surface Adsorptive Additive. *Small* **2024**, *20*, 2406871. [CrossRef] [PubMed]
102. Li, Q.; Wang, C.; Du, W.; Zhu, Y.; Yao, M.; Wang, Y.; Feng, S.; Chen, R. Dynamic Interface Layer Regulation with Extremely Low Content of Chitosan Additive Enables Stable Zinc Metal Anode. *J. Power Sources* **2025**, *625*, 235673. [CrossRef]
103. Gan, Y.; Zeng, J.; Li, H.; Xu, Z.; Shang, B.; Xie, Z.; Li, W. Stable Zinc Anode Achieved through Ultramicro Long Chain Cationic Surfactant as Interface Regulator in Aqueous Electrolyte. *J. Mol. Liq.* **2023**, *390*, 122988. [CrossRef]
104. Yuan, Y.; Pu, S.D.; Pérez-Osorio, M.A.; Li, Z.; Zhang, S.; Yang, S.; Liu, B.; Gong, C.; Menon, A.S.; Piper, L.F.J.; et al. Diagnosing the Electrostatic Shielding Mechanism for Dendrite Suppression in Aqueous Zinc Batteries. *Adv. Mater.* **2024**, *36*, 2307708. [CrossRef] [PubMed]
105. Cheng, Y.; Jiao, Y.; Wu, P. Manipulating Zn 002 Deposition Plane with Zirconium Ion Crosslinked Hydrogel Electrolyte toward Dendrite Free Zn Metal Anodes. *Energy Environ. Sci.* **2023**, *16*, 4561–4571. [CrossRef]
106. Zhang, W.; Dai, Y.; Chen, R.; Xu, Z.; Li, J.; Zong, W.; Li, H.; Li, Z.; Zhang, Z.; Zhu, J.; et al. Highly Reversible Zinc Metal Anode in a Dilute Aqueous Electrolyte Enabled by a pH Buffer Additive. *Angew. Chem. Int. Ed.* **2023**, *62*, e202212695. [CrossRef] [PubMed]

107. Yang, S.; Zhao, S.; Xu, H.; Wang, X.; Huang, X.; Yang, Q.; Chen, Y.; Wang, G.; Chen, S. Gradient Chaotropic Regulation of Zn^{2+} Solvation Chemistry for Low-Temperature Zinc Metal Batteries. *Nat. Commun.* **2025**, *17*, 736. [CrossRef] [PubMed]
108. Chen, B.; Chao, D.; Liu, E.; Jaroniec, M.; Zhao, N.; Qiao, S.-Z. Transition Metal Dichalcogenides for Alkali Metal Ion Batteries: Engineering Strategies at the Atomic Level. *Energy Environ. Sci.* **2020**, *13*, 1096–1131. [CrossRef]
109. Luo, R.; Yang, Q.; Sun, L.; Liu, Y.; Li, L.; Lei, Y.; Shi, W. V_2 O_3 with Se-Enhanced D-p Orbital Hybridization Toward Highly Stable Aqueous Zinc Batteries under 10 A g^{-1}. *Adv. Mater.* **2026**, *38*, e16093. [CrossRef] [PubMed]
110. Kumari, P.; Kundu, R. Zinc-Ion Batteries: Promise and Challenges for Exploring the Post-Lithium Battery Materials. *ACS Appl. Energy Mater.* **2024**, *7*, 9634–9669. [CrossRef]
111. Wang, Y.; Wang, Z.; Pang, W.K.; Lie, W.; Yuwono, J.A.; Liang, G.; Liu, S.; Angelo, A.M.D.; Deng, J.; Fan, Y.; et al. Solvent Control of Water O−H Bonds for Highly Reversible Zinc Ion Batteries. *Nat. Commun.* **2023**, *14*, 2720. [CrossRef] [PubMed]
112. Li, C.; Zhang, X.; Qu, G.; Zhao, S.; Qin, H.; Li, D.; Li, N.; Wang, C.; Xu, X. Highly Reversible Zn Metal Anode Securing by Functional Electrolyte Modulation. *Adv. Energy Mater.* **2024**, *14*, 2400872. [CrossRef]
113. Yoo, G.; Lee, Y.-G.; Im, B.; Kim, D.G.; Jo, Y.-R.; An, G. Integrated Solution for a Stable and High-Performance Zinc-Ion Battery Using an Electrolyte Additive. *Energy Storage Mater.* **2023**, *61*, 102845. [CrossRef]
114. Zhang, R.; Cui, Y.; Liu, L.; Chen, S. A Dual-Functional Rare Earth Halide Additive for High-Performance Aqueous Zinc Ion Batteries. *J. Power Sources* **2024**, *602*, 234351. [CrossRef]
115. Yang, X.; Tang, X.; Lei, J.; Zeng, X.; Wen, J.; Liu, A.; Xia, S.; Luo, Q.; Liu, J.; Xue, A.; et al. A Fluorine-Free Organic/Inorganic Interphase for Highly Reversible Aqueous Zinc Batteries. *Angew. Chem. Int. Ed.* **2025**, *64*, e202504003. [CrossRef] [PubMed]
116. Wu, H.; Yan, W.; Xing, Y.; Li, L.; Liu, J.; Li, L.; Huang, P.; Lai, C.; Wang, C.; Chen, W.; et al. Tailoring the Interfacial Electric Field Using Silicon Nanoparticles for Stable Zinc-ion Batteries. *Adv. Funct. Mater.* **2024**, *34*, 2213882. [CrossRef]
117. Zampardi, G.; La Mantia, F. Open Challenges and Good Experimental Practices in the Research Field of Aqueous Zn-Ion Batteries. *Nat. Commun.* **2022**, *13*, 687. [CrossRef] [PubMed]
118. Yuan, Y.; Sharpe, R.; He, K.; Li, C.; Saray, M.T.; Liu, T.; Yao, W.; Cheng, M.; Jin, H.; Wang, S.; et al. Understanding Intercalation Chemistry for Sustainable Aqueous Zinc–Manganese Dioxide Batteries. *Nat. Sustain.* **2022**, *5*, 890–898. [CrossRef]
119. Deng, R.; Chen, J.; Chu, F.; Qian, M.; He, Z.; Robertson, A.W.; Maier, J.; Wu, F. "Soggy-Sand" Chemistry for High-Voltage Aqueous Zinc-Ion Batteries. *Adv. Mater.* **2024**, *36*, 2311153. [CrossRef] [PubMed]
120. Wu, W.; Gao, H.; Jia, L.; Li, Y.; Zhang, D.; Zhan, H.; Xu, J.; Li, B.; Geng, Z.; Cheng, Y.; et al. Stable and Uniform Self-Assembled Organic Diradical Molecules for Perovskite Photovoltaics. *Science* **2025**, *389*, 195–199. [CrossRef] [PubMed]
121. Wang, H.; Deng, S.; Wang, S.; Li, W.; Yuan, S.; Han, J.; Fu, H.; Xu, B.; Wei, L. High-Entropy Electrolytes with High Disordered Solvation Structures for Ultra-Stable Zinc Metal Anodes. *Angew. Chem. Int. Ed.* **2025**, *64*, e202422395. [CrossRef] [PubMed]
122. Tang, M.; Liu, Q.; Zou, X.; Zhang, B.; An, L. High-Energy-Density Aqueous Zinc-Ion Batteries: Recent Progress, Design Strategies, Challenges, and Perspectives. *Adv. Mater.* **2025**, *37*, 2501361. [CrossRef] [PubMed]
123. Zhao, K.; Fan, G.; Liu, J.; Liu, F.; Li, J.; Zhou, X.; Ni, Y.; Yu, M.; Zhang, Y.-M.; Su, H.; et al. Boosting the Kinetics and Stability of Zn Anodes in Aqueous Electrolytes with Supramolecular Cyclodextrin Additives. *J. Am. Chem. Soc.* **2022**, *144*, 11129–11137. [CrossRef] [PubMed]
124. Xia, H.; Xu, G.; Cao, X.; Miao, C.; Zhang, H.; Chen, P.; Zhou, Y.; Zhang, W.; Sun, Z. Single-Ion-Conducting Hydrogel Electrolytes Based on Slide-Ring Pseudo-Polyrotaxane for Ultralong-Cycling Flexible Zinc-Ion Batteries. *Adv. Mater.* **2023**, *35*, 2301996. [CrossRef] [PubMed]
125. Lin, D.; Lin, Y.; Pan, R.; Li, J.; Zhu, A.; Zhang, T.; Liu, K.; Feng, D.; Liu, K.; Zhou, Y.; et al. Water-Restrained Hydrogel Electrolytes with Repulsion-Driven Cationic Express Pathways for Durable Zinc-Ion Batteries. *Nano-Micro Lett.* **2025**, *17*, 193. [CrossRef] [PubMed]
126. Qin, Y.; Li, H.; Han, C.; Mo, F.; Wang, X. Chemical Welding of the Electrode–Electrolyte Interface by Zn-Metal-Initiated In Situ Gelation for Ultralong-Life Zn-Ion Batteries. *Adv. Mater.* **2022**, *34*, 2207118. [CrossRef] [PubMed]
127. Jin, S.; Yin, J.; Gao, X.; Sharma, A.; Chen, P.; Hong, S.; Zhao, Q.; Zheng, J.; Deng, Y.; Joo, Y.L.; et al. Production of Fast-Charge Zn-Based Aqueous Batteries via Interfacial Adsorption of Ion-Oligomer Complexes. *Nat. Commun.* **2022**, *13*, 2283. [CrossRef] [PubMed]
128. Shinde, P.A.; Chodankar, N.R.; Shrestha, L.K.; Al Ghaferi, A.; Alhajri, E.; Ariga, K. Stable and Dendrite-Free Zinc Metal Anodes Via Interface Nanoarchitectonics for Aqueous Zinc-Ion Batteries. *Adv. Funct. Mater.* **2025**, *35*, e2424242. [CrossRef]
129. Wang, B.; Guan, C.; Zhou, Q.; Wang, Y.; Zhu, Y.; Bian, H.; Chen, Z.; Zhang, S.; Tan, X.; Luo, B.; et al. Screening Anionic Groups Within Zwitterionic Additives for Eliminating Hydrogen Evolution and Dendrites in Aqueous Zinc Ion Batteries. *Nano-Micro Lett.* **2025**, *17*, 314. [CrossRef] [PubMed]
130. Cai, Z.; Wang, J.; Lian, S.; Chen, J.; Lang, F.; Li, Z.; Li, Q. Regulating the Zn Electrode/Electrolyte Interface Toward High Stability–Insights from the Resting Time Impact on Zn Electrode Performance. *Adv. Funct. Mater.* **2025**, *35*, 2401367. [CrossRef]
131. Chao, D.; Zhou, W.; Xie, F.; Ye, C.; Li, H.; Jaroniec, M.; Qiao, S.-Z. Roadmap for Advanced Aqueous Batteries: From Design of Materials to Applications. *Sci. Adv.* **2020**, *6*, eaba4098. [CrossRef] [PubMed]

132. Geng, H.; Cheng, M.; Wang, B.; Yang, Y.; Zhang, Y.; Li, C.C. Electronic Structure Regulation of Layered Vanadium Oxide via Interlayer Doping Strategy toward Superior High-Rate and Low-Temperature Zinc-Ion Batteries. *Adv. Funct. Mater.* **2020**, *30*, 1907684. [CrossRef]
133. Chen, M.; Guo, X.; Jiang, X.; Farhadi, B.; Guo, X.; Zhu, Y.; Zhang, H.; Liu, S. (Frank) Multi-Group Polymer Coating on Zn Anode for High Overall Conversion Efficiency Photorechargeable Zinc-Ion Batteries. *Angew. Chem. Int. Ed.* **2024**, *63*, e202410011. [CrossRef] [PubMed]
134. Xia, H.; Shui, T.; Wan, X.; Chen, Y.; Wang, F.; Miao, C.; Cao, X.; Pan, B.; Pan, Z.; Xie, Q.; et al. Microphase-Separated Hydrogel Electrolytes with Selective Ion Transportation Pathways for Flexible Zinc-Ion Batteries. *Adv. Mater.* **2026**, *38*, e18881. [CrossRef] [PubMed]
135. Konarov, A.; Voronina, N.; Jo, J.H.; Bakenov, Z.; Sun, Y.-K.; Myung, S.-T. Present and Future Perspective on Electrode Materials for Rechargeable Zinc-Ion Batteries. *ACS Energy Lett.* **2018**, *3*, 2620–2640. [CrossRef]
136. Wei, Y.; Wang, B.; Qian, Z.; Pan, H.; Peng, Z.; Sun, Y.; Yao, X. Promoting Zn^{2+} Interfacial Transfer and (002)-Textured Zn Deposition via a Thin AlF3 Layer for Stable Zn Electrode in Aqueous Battery. *Small Methods* **2025**, *9*, e01277. [CrossRef] [PubMed]
137. Cao, J.; Zhang, D.; Yue, Y.; Chanajaree, R.; Wang, S.; Han, J.; Zhang, X.; Qin, J.; Huang, Y. Regulating Solvation Structure to Stabilize Zinc Anode by Fastening the Free Water Molecules with an Inorganic Colloidal Electrolyte. *Nano Energy* **2022**, *93*, 106839. [CrossRef]
138. Verma, V.; Chan, R.M.; Jia Yang, L.; Kumar, S.; Sattayaporn, S.; Chua, R.; Cai, Y.; Kidkhunthod, P.; Manalastas, W., Jr.; Srinivasan, M. Chelating Ligands as Electrolyte Solvent for Rechargeable Zinc-Ion Batteries. *Chem. Mater.* **2021**, *33*, 1330–1340. [CrossRef]
139. Yang, Z.; Li, W.; Zhang, Q.; Xie, C.; Ji, H.; Tang, Y.; Li, Y.; Wang, H. A Piece of Common Cellulose Paper but with Outstanding Functions for Advanced Aqueous Zinc-Ion Batteries. *Mater. Today Energy* **2022**, *28*, 101076. [CrossRef]
140. Zhang, N.; Cheng, F.; Liu, Y.; Zhao, Q.; Lei, K.; Chen, C.; Liu, X.; Chen, J. Cation-Deficient Spinel $ZnMn_2O_4$ Cathode in $Zn(CF_3SO_3)_2$ Electrolyte for Rechargeable Aqueous Zn-Ion Battery. *J. Am. Chem. Soc.* **2016**, *138*, 12894–12901. [CrossRef] [PubMed]
141. Yadav, G.G.; Turney, D.; Huang, J.; Wei, X.; Banerjee, S. Breaking the 2 V Barrier in Aqueous Zinc Chemistry: Creating 2.45 and 2.8 V MnO_2–Zn Aqueous Batteries. *ACS Energy Lett.* **2019**, *4*, 2144–2146. [CrossRef]
142. Yan, T.; Wang, L.; Huang, S.; Shen, S.; Zhang, L. Competitive Coordination Enables Aqueous Four-Electron Zinc-Iodine Batteries over 60,000 Cycles. *Energy Storage Mater.* **2026**, *84*, 104837. [CrossRef]
143. Huang, C.; Zhao, X.; Hao, Y.; Yang, Y.; Qian, Y.; Chang, G.; Zhang, Y.; Tang, Q.; Hu, A.; Chen, X. Long Shelf-Life Efficient Electrolytes Based on Trace l-Cysteine Additives toward Stable Zinc Metal Anodes. *Small* **2022**, *18*, 2203674. [CrossRef] [PubMed]
144. Nian, Q.; Luo, X.; Ruan, D.; Li, Y.; Xiong, B.-Q.; Cui, Z.; Wang, Z.; Dong, Q.; Fan, J.; Jiang, J.; et al. Highly Reversible Zinc Metal Anode Enabled by Strong Brønsted Acid and Hydrophobic Interfacial Chemistry. *Nat. Commun.* **2024**, *15*, 4303. [CrossRef] [PubMed]
145. Ma, L.; Pollard, T.P.; Zhang, Y.; Schroeder, M.A.; Ding, M.S.; Cresce, A.V.; Sun, R.; Baker, D.R.; Helms, B.A.; Maginn, E.J.; et al. Functionalized Phosphonium Cations Enable Zinc Metal Reversibility in Aqueous Electrolytes. *Angew. Chem.* **2021**, *133*, 12546–12553. [CrossRef] [PubMed]
146. Xu, M.; Li, J.; Wang, L.; Wang, Z.; Wang, M.; Li, L.; Cai, X.; Li, L.; Shangguan, E. Engineering Sb/Zn4(OH)6SO4·5H2O Interfacial Layer by in Situ Chemically Reacting for Stable Zn Anode. *J. Colloid. Interface Sci.* **2024**, *671*, 742–750. [CrossRef] [PubMed]
147. Li, C.; Shyamsunder, A.; Hoane, A.G.; Long, D.M.; Kwok, C.Y.; Kotula, P.G.; Zavadil, K.R.; Gewirth, A.A.; Nazar, L.F. Highly Reversible Zn Anode with a Practical Areal Capacity Enabled by a Sustainable Electrolyte and Superacid Interfacial Chemistry. *Joule* **2022**, *6*, 1103–1120. [CrossRef]
148. Chen, D.; Lu, M.; Cai, D.; Yang, H.; Han, W. Recent Advances in Energy Storage Mechanism of Aqueous Zinc-Ion Batteries. *J. Energy Chem.* **2021**, *54*, 712–726. [CrossRef]
149. Xie, X.; Deng, L.; Li, L.; Pan, A.; Liang, S.; Fang, G. Modulating Interfacial Zn^{2+} Deposition Mode towards Stable Zn Anode via Bimetallic Co-Doped Coating. *Energy Storage Mater.* **2024**, *73*, 103834. [CrossRef]
150. Aupama, V.; Kao-ian, W.; Sangsawang, J.; Mohan, G.; Wannapaiboon, S.; Mohamad, A.A.; Pattananuwat, P.; Sriprachuabwong, C.; Liu, W.-R.; Kheawhom, S. Stabilizing a Zinc Anode via a Tunable Covalent Organic Framework-Based Solid Electrolyte Interphase. *Nanoscale* **2023**, *15*, 9003–9013. [CrossRef] [PubMed]
151. Zheng, J.; Yin, J.; Zhang, D.; Li, G.; Bock, D.C.; Tang, T.; Zhao, Q.; Liu, X.; Warren, A.; Deng, Y.; et al. Spontaneous and Field-Induced Crystallographic Reorientation of Metal Electrodeposits at Battery Anodes. *Sci. Adv.* **2020**, *6*, eabb1122. [CrossRef] [PubMed]
152. Roy, K.; Rana, A.; Heil, J.N.; Tackett, B.M.; Dick, J.E. For Zinc Metal Batteries, How Many Electrons Go to Hydrogen Evolution? An Electrochemical Mass Spectrometry Study. *Angew. Chem. Int. Ed.* **2024**, *136*, e202319010. [CrossRef]
153. Huth, E. Propeller Meters Prove Economical and Durable. *Opflow* **1990**, *16*, 1–5. [CrossRef]
154. Ren, J.; Zhang, J.; Chen, Y.; Liu, R.; Liu, C.; Guo, X.; Luo, D.; Wang, D.; Chen, Z. Multiphase Aqueous Soggy Sand Electrolyte for Zinc Metal Batteries Applications at Elevated Temperatures. *Nat. Commun.* **2025**, *17*, 309. [CrossRef] [PubMed]

155. Yuksel, R.; Buyukcakir, O.; Seong, W.K.; Ruoff, R.S. Metal-Organic Framework Integrated Anodes for Aqueous Zinc-Ion Batteries. *Adv. Energy Mater.* **2020**, *10*, 1904215. [CrossRef]
156. Innocenti, A.; Bresser, D.; Garche, J.; Passerini, S. A Critical Discussion of the Current Availability of Lithium and Zinc for Use in Batteries. *Nat. Commun.* **2024**, *15*, 4068. [CrossRef] [PubMed]
157. Naveed, A.; Yang, H.; Shao, Y.; Yang, J.; Yanna, N.; Liu, J.; Shi, S.; Zhang, L.; Ye, A.; He, B.; et al. A Highly Reversible Zn Anode with Intrinsically Safe Organic Electrolyte for Long-Cycle-Life Batteries. *Adv. Mater.* **2019**, *31*, 1900668. [CrossRef] [PubMed]

Disclaimer/Publisher's Note: The statements, opinions and data contained in all publications are solely those of the individual author(s) and contributor(s) and not of MDPI and/or the editor(s). MDPI and/or the editor(s) disclaim responsibility for any injury to people or property resulting from any ideas, methods, instructions or products referred to in the content.